

NATIONAL ADVISORY COMMITTEE FOR AERONAUTICS

TECHNICAL NOTE

No. 1052

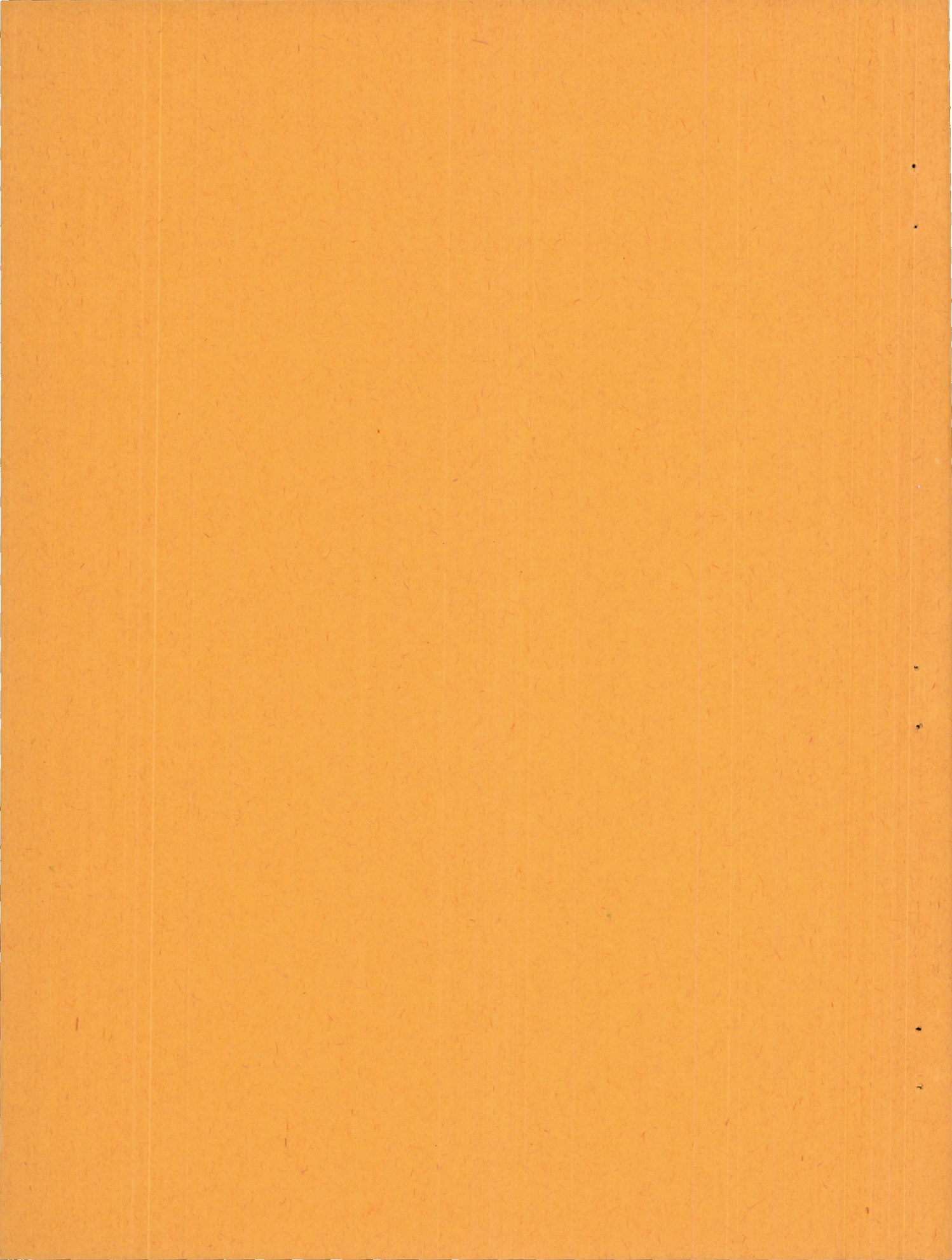
WIND-TUNNEL INVESTIGATION OF EFFECT OF CANOPIES
ON DIRECTIONAL STABILITY CHARACTERISTICS
OF A SINGLE-ENGINE AIRPLANE MODEL

By Robert MacLachlan and Joseph Levitt

Langley Memorial Aeronautical Laboratory
Langley Field, Va.



Washington
May 1946



NATIONAL ADVISORY COMMITTEE FOR AERONAUTICS

TECHNICAL NOTE NO. 1052

WIND-TUNNEL INVESTIGATION OF EFFECT OF CANOPIES
ON DIRECTIONAL STABILITY CHARACTERISTICS
OF A SINGLE-ENGINE AIRPLANE MODEL

By Robert MacLachlan and Joseph Levitt

SUMMARY

A low-wing, single-engine airplane model was tested in the Langley stability tunnel to obtain data showing the effect of canopy size and shape on the directional stability characteristics of the model.

In general, the addition of a canopy to the model decreased the directional stability of the model. Destabilizing interference between a canopy and the model with vertical tail off resulted from the addition to the model of only the two largest canopies tested. Only the largest and least streamlined canopy tested showed appreciable canopy vertical-tail interference at low angles of attack. As the angle of attack increased, however, all the canopies tested reduced the vertical-tail effectiveness, the reduction being approximately proportional to the vertical-tail area. When the fuselage length was increased, the decrease in directional stability resulting from the addition of a canopy to the model with vertical tail on became smaller at low angles of attack and larger at high angles of attack.

INTRODUCTION

A recent unpublished investigation based on flight results indicated that interference of a canopy on the vertical tail of an airplane might seriously affect the directional stability of the airplane. The limited amount of data available, however, did not permit an adequate determination of canopy-tail interference.

The present investigation was made to obtain data showing the effect of canopy shape and size on the directional stability of a low-wing, single-engine airplane model. In order to cover a wide range of canopy size, two of the four canopies tested were larger and two were smaller than would be expected for a conventional fighter-type airplane. In addition to variations in size and shape of canopy, the tests included changes in vertical-tail area and fuselage length.

APPARATUS AND MODEL

The tests were conducted in the 6- by 6-foot test section of the Langley stability tunnel. The model was mounted on a three-strut support (fig. 1), and force and moment readings were obtained from the tunnel balances. A three-view drawing of the model is given as figure 2. The fuselage was of circular cross section and its length was changed by the use of three interchangeable tail cones. (See fig. 2.)

The four canopies used in the present investigation have been designated the small bubble canopy (fig. 1(a)), the small box canopy (fig. 1(b)), the large bubble canopy (fig. 1(c)), and the large box canopy (fig. 1(d)). For one test the large bubble canopy was cut and the rear portion moved back to simulate an open canopy (fig. 1(e)). The two large canopies are the same in frontal area and shape and, in like respects, the two small canopies are identical. A line drawing of the model showing the various canopies is given as figure 3.

Three geometrically similar vertical tail surfaces conforming to the NACA 0009 airfoil section were used. The aspect ratio of each of the vertical tails was 2.15; the vertical tails were installed on the model at 0° angle of incidence relative to the plane of symmetry of the model. The horizontal tail of the model also conformed to the NACA 0009 airfoil section but had an aspect ratio of 4.0. The dimensions of all the tail surfaces are presented in table I and figure 2.

TESTS

The model configurations tested are given in table II. The model was tested through an angle-of-attack range

from about -5° to 10° at angles of yaw of $\pm 2^\circ$ and through an angle-of-yaw range from -10° to 20° at angles of attack of about 0° and 10° . All tests were made with the propeller windmilling. The dynamic pressure was 64.3 pounds per square foot. The corresponding airspeed under standard sea-level atmospheric conditions was 159 miles per hour and the Reynolds number based on the mean wing chord of the model (8.73 in.) was about 1.1×10^6 . The Mach number was approximately 0.21.

PRESENTATION OF DATA

The results of the tests are presented in standard NACA coefficient form in figures 4 to 9. The pitching-moment, rolling-moment, and yawing-moment coefficients are given about the center-of-gravity location shown in figure 2. The data are referred to the stability axes, which are a system of axes having their origin at the center of gravity and in which the Z-axis is in the plane of symmetry and perpendicular to the relative wind, the X-axis is in the plane of symmetry and perpendicular to the Z-axis, and the Y-axis is perpendicular to the plane of symmetry.

The coefficients and symbols used are defined as follows:

$$C_L \quad \text{lift coefficient} \left(\frac{\text{Lift}}{qS_w} \right)$$

$$C_D \quad \text{total drag coefficient} \left(\frac{\text{Drag}}{qS_w} \right)$$

$$C_Y \quad \text{lateral-force coefficient} \left(\frac{Y}{qS_w} \right)$$

$$C_l \quad \text{rolling-moment coefficient} \left(\frac{L}{qS_w b} \right)$$

$$C_m \quad \text{pitching-moment coefficient} \left(\frac{M}{qS_w c} \right)$$

$$C_n \quad \text{yawing-moment coefficient} \left(\frac{N}{qS_w b} \right)$$

$$C_{n\psi} = \frac{\partial C_n}{\partial \psi}$$

- ΔC_n increment of C_n resulting from addition of canopy to model
- $\Delta C_{n\psi}$ slope of curve of ΔC_n against ψ at $\psi = 0^\circ$ $\left(\frac{\partial(\Delta C_n)}{\partial\psi} \right)$
- Y force along Y-axis; positive when acting to the right
- L moment about X-axis; positive when it tends to depress right wing
- M moment about Y-axis; positive when it tends to raise nose
- N moment about Z-axis; positive when it tends to turn nose to right
- q dynamic pressure, pounds per square foot $\left(\frac{1}{2} \rho V^2 \right)$
- V free-stream velocity, feet per second
- ρ mass density of air, slugs per cubic foot
- S_w wing area (2.625 sq ft)
- b wing span (4 ft)
- c airfoil section chord, feet
- \bar{c} mean aerodynamic chord $\left(\frac{2}{S} \int_0^{b/2} c^2 db = 0.728 \text{ ft} \right)$
- S_v vertical-tail area, square feet
- α angle of attack of fuselage center line, degrees
- ψ angle of yaw, degrees

The accuracies of C_n , C_l , and C_y were determined experimentally to be about ± 0.001 , ± 0.0016 , and ± 0.002 , respectively. The accuracies of the angle-of-attack and angle-of-yaw measurements were about $\pm 0.1^\circ$ and $\pm 0.05^\circ$, respectively. Since the accuracy of C_n was about ± 0.001 , the accuracy of ΔC_n (the computation of which involved the subtraction of two C_n -values) was only ± 0.002 . The subsequent fairing of the curves of ΔC_n against ψ was believed justifiable although some of the points fell outside the ± 0.002 limits.

The corrections to angle of attack and drag coefficients for tunnel-wall effect were computed by the following formulas:

$$\begin{aligned}\Delta\alpha &= 57.3\delta_w \frac{S_w}{C} C_L \\ &= 0.637C_L\end{aligned}$$

$$\begin{aligned}\Delta C_D &= \delta_w \frac{S_w}{C} C_L^2 \\ &= 0.011C_L^2\end{aligned}$$

where δ_w is the jet-boundary correction factor at the wing (0.1525) and C is the cross-sectional area of the tunnel (36 sq ft). Both corrections were additive. No tare tests were made and no jet-boundary corrections were applied to the other coefficients.

DISCUSSION

Effect of Large Box Canopy on Lift, Drag, and Pitching-Moment Coefficients

The effect of the large box canopy on the lift, drag, and pitching-moment coefficients of the model is shown in figure 4. The lift coefficients were the same for both canopy-off and canopy-on conditions. The effect of separation of flow at the wing roots, which was observed in tuft tests of a previous investigation, can be seen in the preliminary rounding off of the lift curve at angles of attack of about 13° . Without fillets at the wing-fuselage junction, this separation occurred at an angle of attack between 8° and 10° . The canopy apparently did not affect the angle at which separation occurred. With the canopy on, the drag coefficient of the model was higher than with the canopy off, as would be expected. At negative and small positive angles of attack, addition of the canopy made the pitching-moment coefficient more positive.

Effect of Canopies on Yawing-Moment Coefficient

The increments of yawing-moment coefficient resulting from the addition of the canopies to the model are shown

in figure 7. The variation of these increments with angle of yaw tended to be destabilizing except at low angles of yaw, where for the small canopies and the large bubble canopy the variation in ΔC_n with ψ frequently appeared to be stabilizing. The values of ΔC_n at low angles of yaw, however, were somewhat erratic; therefore the curves of ΔC_n against ψ were faired linearly from $\psi = -10^\circ$ to $\psi = 10^\circ$. At angles of yaw greater than 10° , the increment of yawing-moment coefficient for the model with vertical tail on tended to decrease as the angle of yaw increased. This effect, which became more pronounced as the vertical-tail area was increased, may be attributed to the departure of the vertical tail from the canopy wake as the angle of yaw increased.

Effect of Change in Canopy Size and Shape on $\Delta C_{n\psi}$

The slopes $\Delta C_{n\psi}$ were measured from the curves in figure 7 and were plotted against the ratio of vertical-tail area to wing area (see fig. 8). In general the canopies tended to decrease the directional stability of the model. The change in $C_{n\psi}$ resulting from the addition of a canopy to the model was greatest for the large box canopy and was progressively less for the large bubble, the small box, and the small bubble canopies. The change in $C_{n\psi}$ when the large box canopy was added to the model amounted in one case to as much as one-fourth of the value obtained for the model with canopy off, whereas the addition of the small bubble canopy had very little effect on $C_{n\psi}$. For the model with vertical tail on, the decrement in directional stability resulting from the addition of a canopy was greater, in almost all cases, at $\alpha = 10.6^\circ$ than at $\alpha = 0.1^\circ$.

In order to determine the effect on the directional stability of the model of opening the large bubble canopy, values of $C_{n\psi}$ as measured from the values of yawing-moment coefficient at $\psi = \pm 2^\circ$ were plotted against angle of attack (fig. 9). The curves thus obtained were considered sufficiently accurate to infer that opening the canopy decreased the directional stability of the model (with tail on) at negative angles of attack but had little effect at angles of attack in the normal landing range.

Effect of Change in Vertical-Tail Area on $\Delta C_{n\psi}$

The interference between the canopies and the model with vertical tail off can be seen in figure 8(a) to be negligible for the two small canopies and greater for the large box canopy than for the large bubble canopy. This interference is slightly less at $\alpha = 10.6^\circ$ than at $\alpha = 0.1^\circ$.

As the vertical-tail area was increased, the value of $\Delta C_{n\psi}$ increased. At an angle of attack of 0.1° , however, the increase in $\Delta C_{n\psi}$ resulting from the addition of a vertical tail to the model or from increase in vertical-tail area was very small for all canopies tested with the exception of the large box canopy (fig. 8(a)). It appears, then, that the interference of the canopy on the vertical tail was serious at low angles of attack only when the large box canopy was attached to the model. At an angle of attack of 10.6° , canopy vertical-tail interference was apparent for all the canopies tested, which indicated that the canopy vertical-tail interference increased as the angle of attack increased positively.

Effect of Changes in Fuselage Length on $\Delta C_{n\psi}$

With vertical tail on, increase in fuselage length decreased the value of $\Delta C_{n\psi}$ for the model at an angle of attack of 0.1° (fig. 8(b)). At an angle of attack of 10.6° , however, increase in fuselage length increased the value of $\Delta C_{n\psi}$. The decrease in $\Delta C_{n\psi}$ with increase in fuselage length at $\alpha = 0.1^\circ$ probably resulted from moving the vertical tail farther from the canopy wake when the model was in a yawed condition. The increase in $\Delta C_{n\psi}$ with increase in fuselage length at $\alpha = 10.6^\circ$ probably resulted from the lowering of the vertical tail farther into the canopy wake as the fuselage length was increased.

CONCLUSIONS

A wind-tunnel investigation of the effect of canopies on directional stability characteristics of a single-engine airplane model indicated the following conclusions:

1. In general, the addition of a canopy to the model decreased the directional stability of the model.

2. Destabilizing interference between a canopy and the model with vertical tail off resulted from the addition to the model of only the two largest canopies tested.

3. Only the largest and least streamlined canopy tested showed appreciable canopy vertical-tail interference at low angles of attack. As the angle of attack increased, however, all the canopies tested reduced the vertical-tail effectiveness, the reduction being approximately proportional to the vertical-tail area.

4. When the fuselage length was increased, the decrease in directional stability resulting from the addition of a canopy to the model with vertical tail on became smaller at low angles of attack and larger at high angles of attack.

Langley Memorial Aeronautical Laboratory
National Advisory Committee for Aeronautics
Langley Field, Va., December 20, 1945

TABLE I

TAIL-SURFACE DIMENSIONS

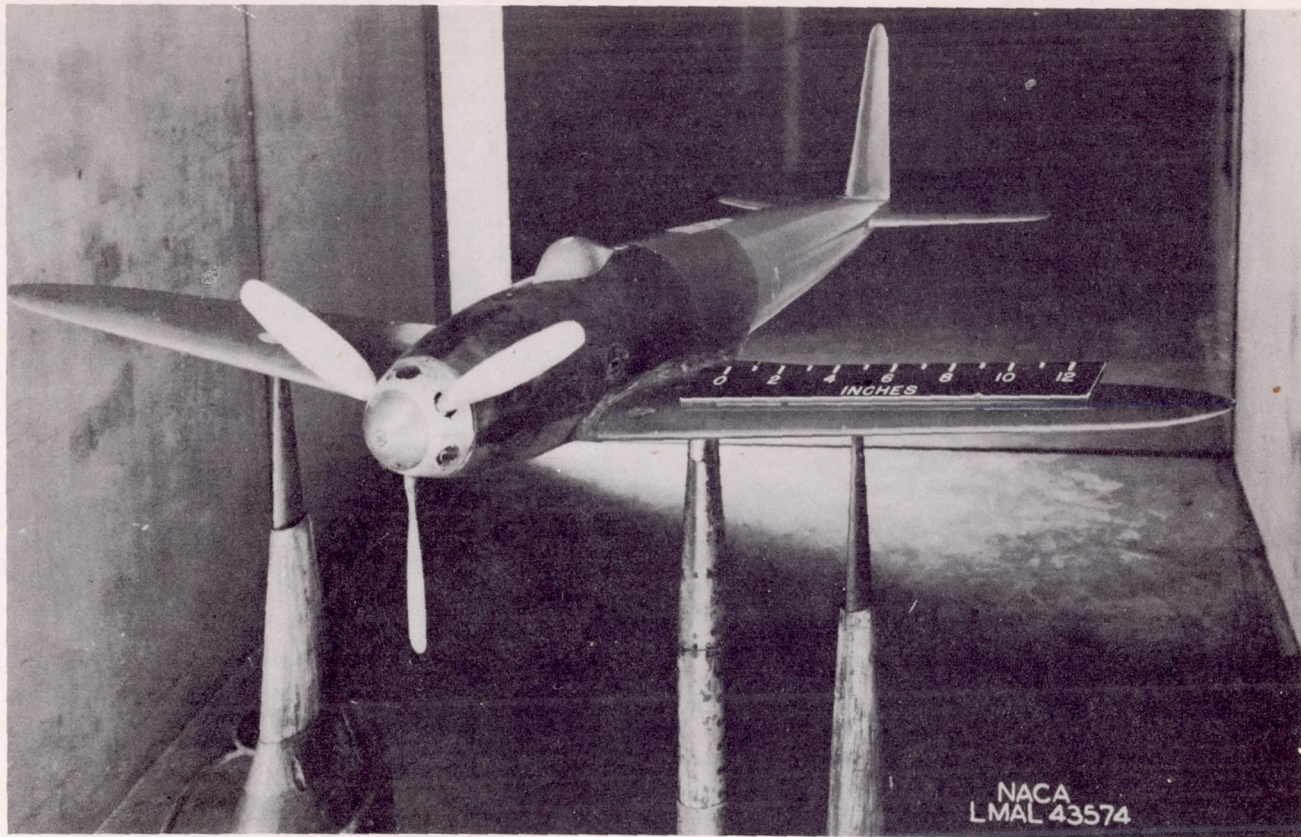
| Tail surface | Designation | Tail area (sq in.) | Tail area / Wing area | Aspect ratio | Taper ratio |
|--------------|-------------|--------------------|-----------------------|--------------|-------------|
| Vertical | 1 | 10.83 | 0.0287 | 2.15 | 2.90:1 |
| Do----- | 2 | 28.37 | .0751 | 2.15 | 2.90:1 |
| Do----- | 3 | 46.20 | .1222 | 2.15 | 2.90:1 |
| Horizontal | ----- | 64.21 | .1699 | 3.99 | 2.96:1 |

NATIONAL ADVISORY
COMMITTEE FOR AERONAUTICS

TABLE II

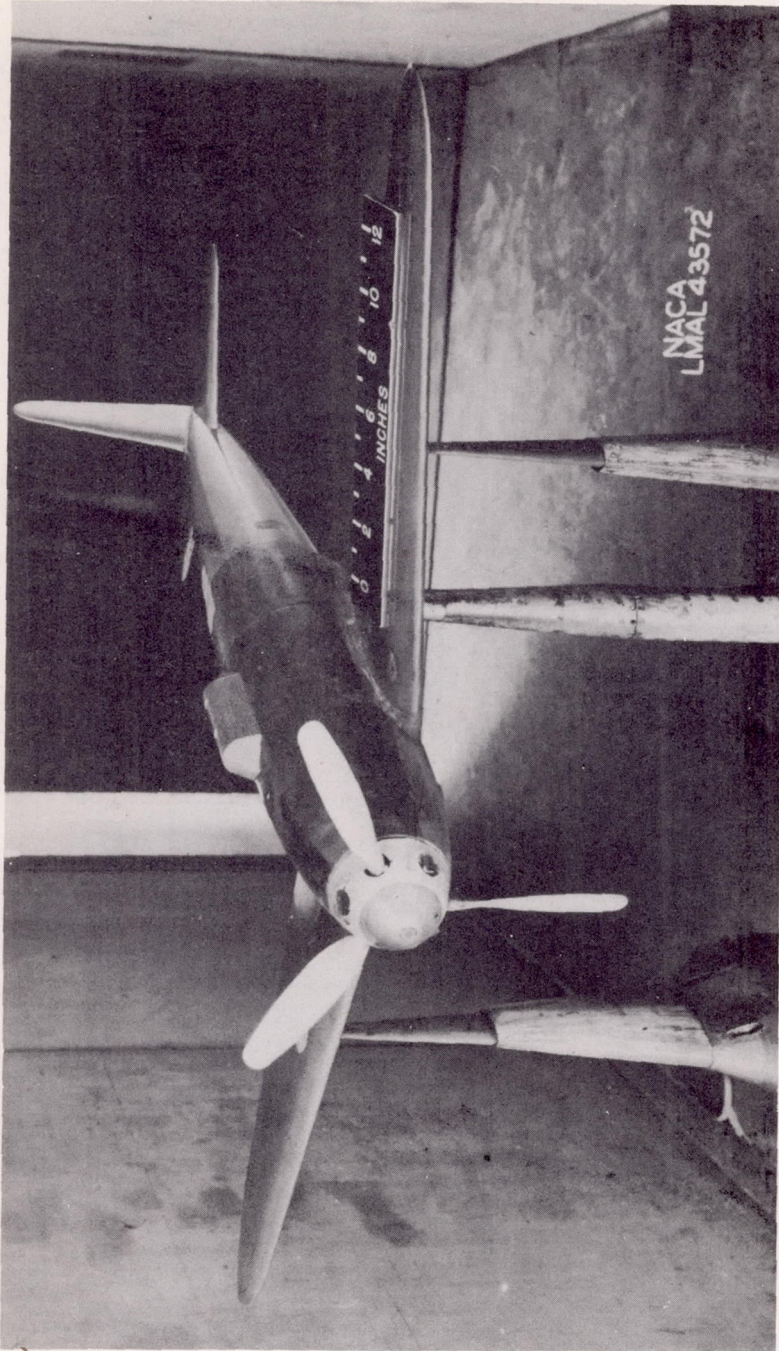
MODEL CONFIGURATIONS TESTED

| Fuselage | Vertical tail | Canopy |
|----------|---------------|--|
| Short | Off | Large box; none |
| | 2 | |
| Medium | Off | Large box; large bubble; small box; small bubble; none |
| | 1 | |
| | 2 | |
| | 3 | |
| Medium | Off | Large bubble open |
| | 2 | |
| Long | Off | Large box; none |
| | 2 | |

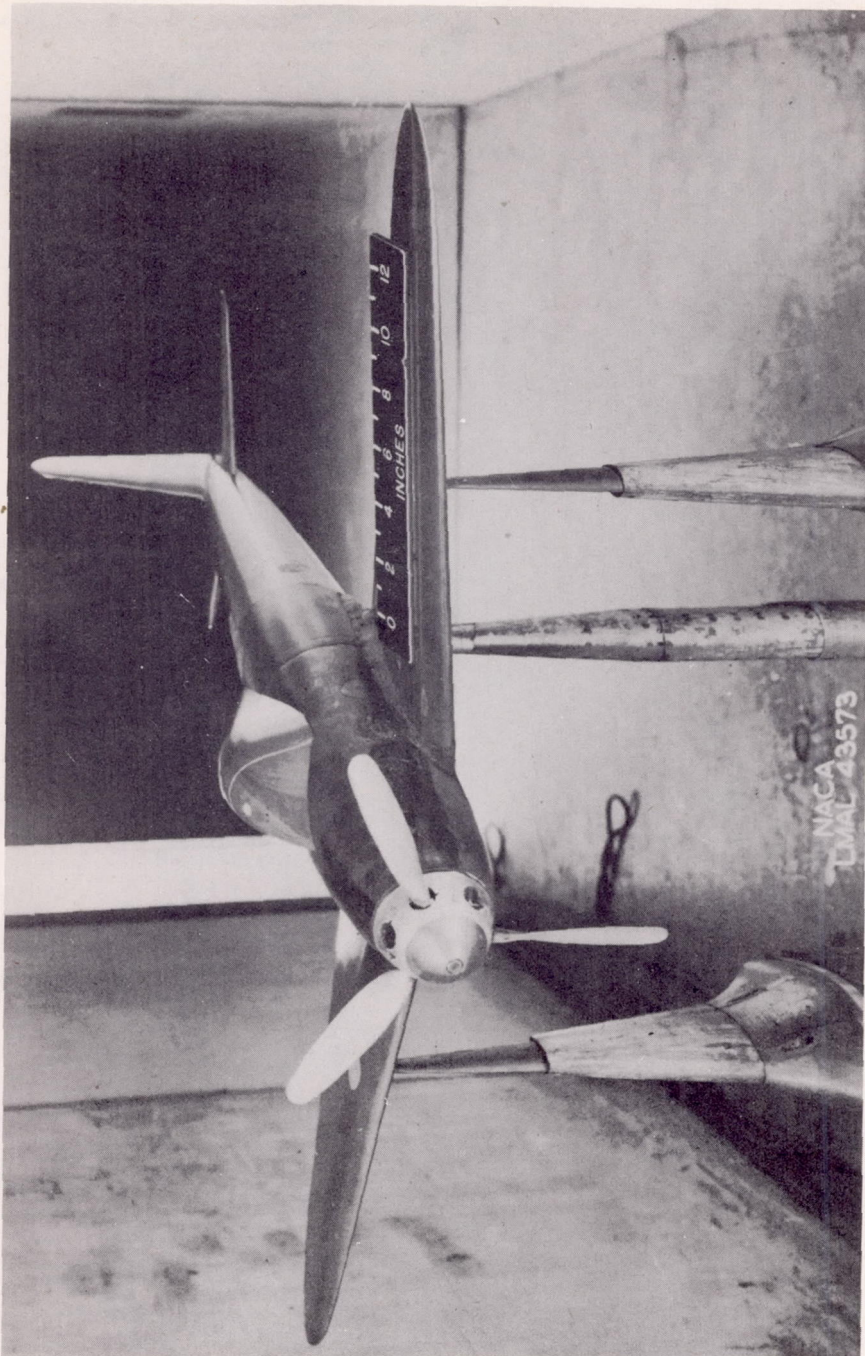


(a) Small bubble canopy.

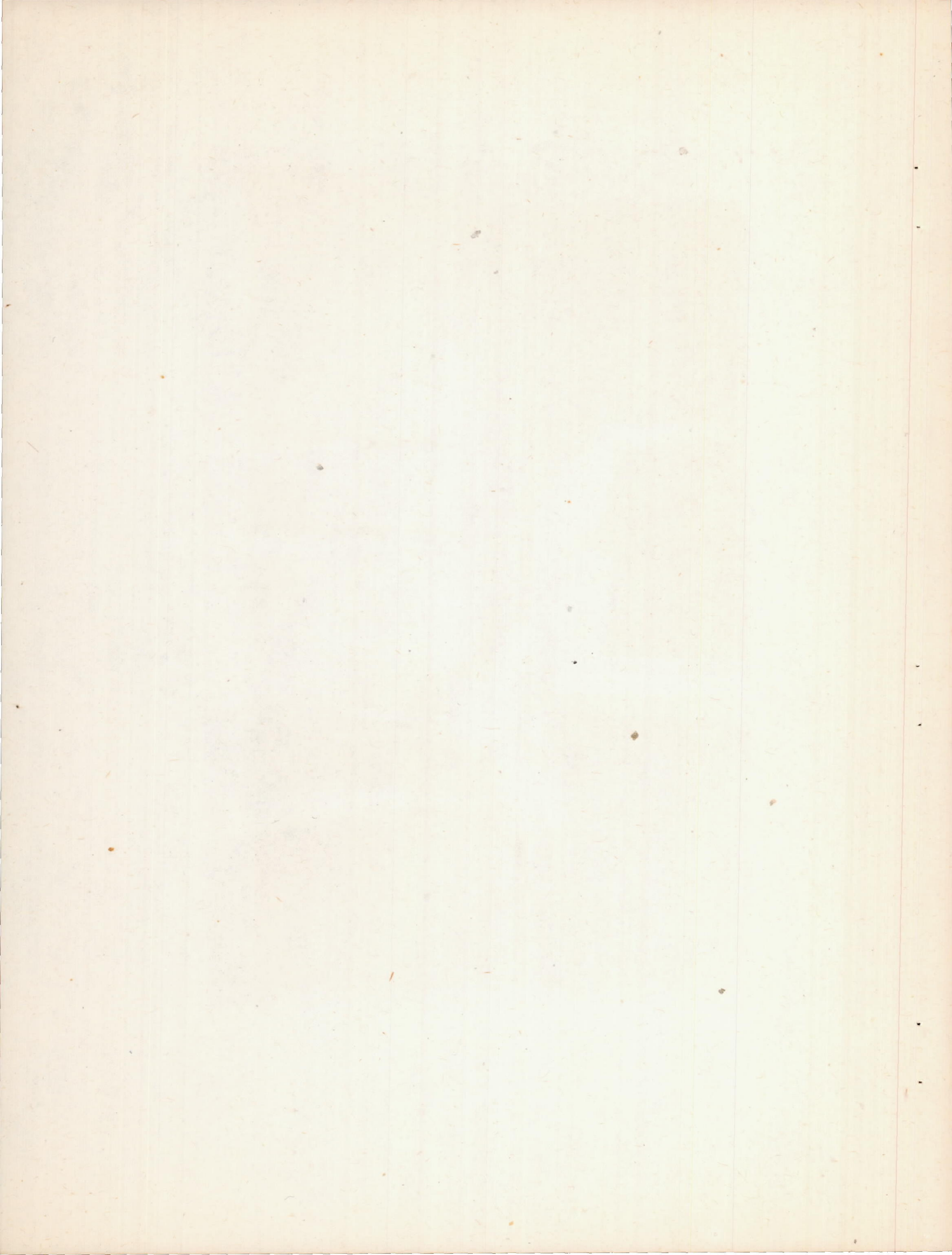
Figure 1.- View of model mounted on three-strut support in Langley stability tunnel.

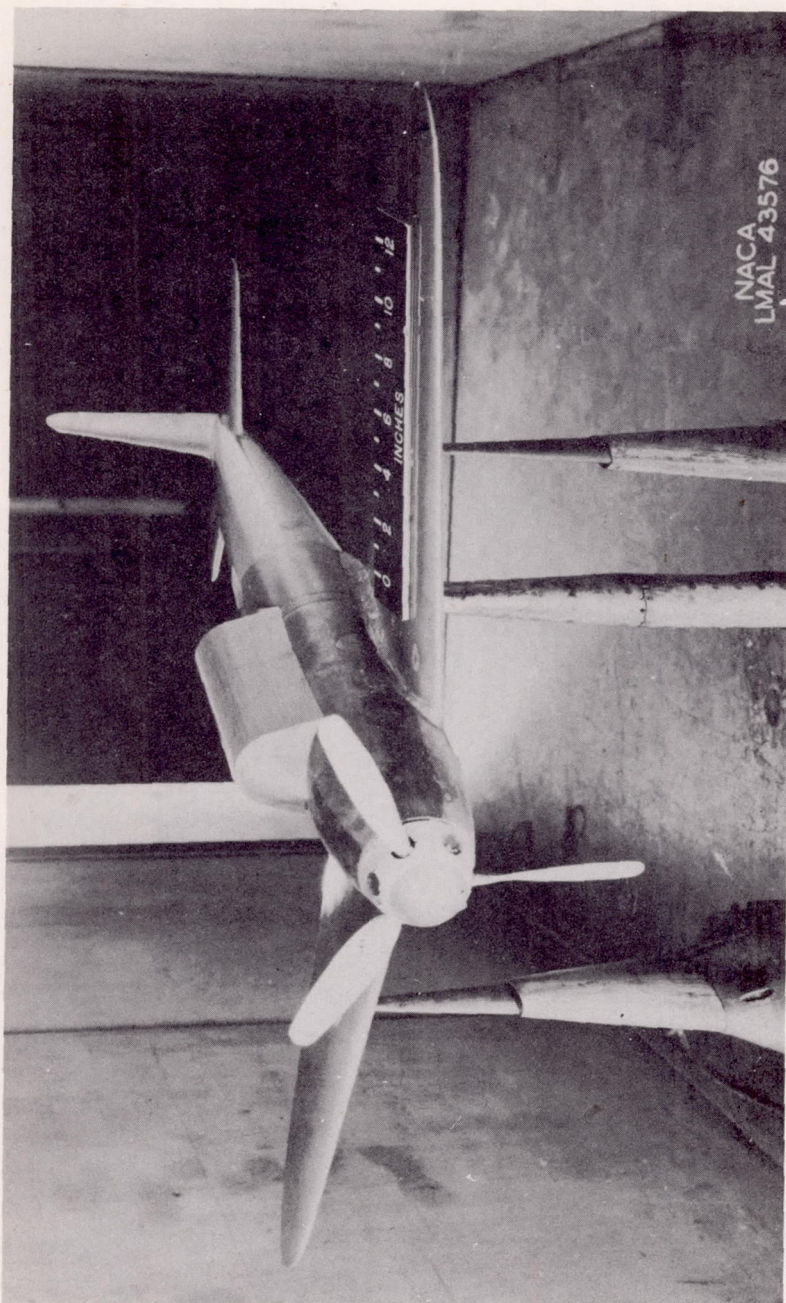


(b) Small box canopy.
Figure 1.- Continued.

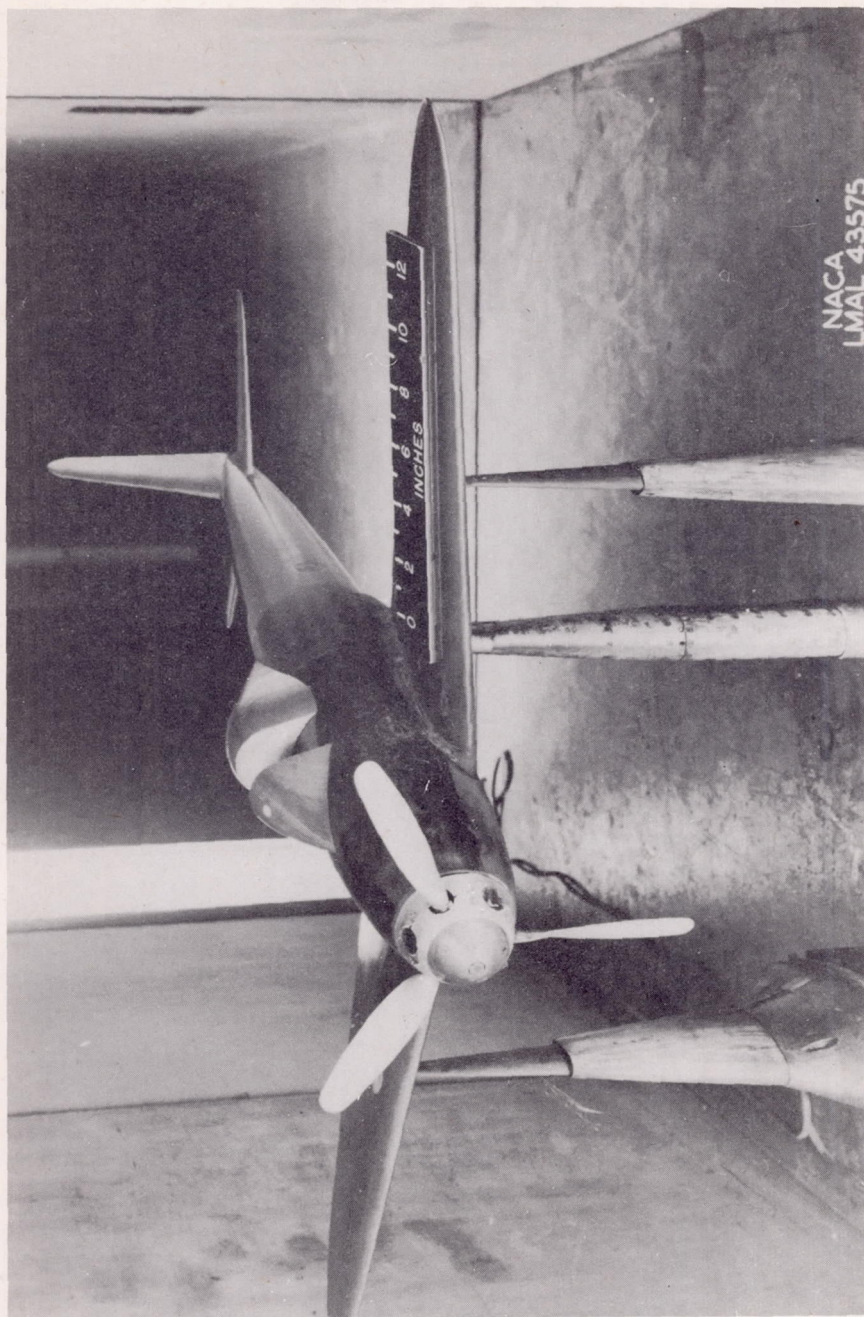


(c) Large bubble canopy.
Figure 1.- Continued.



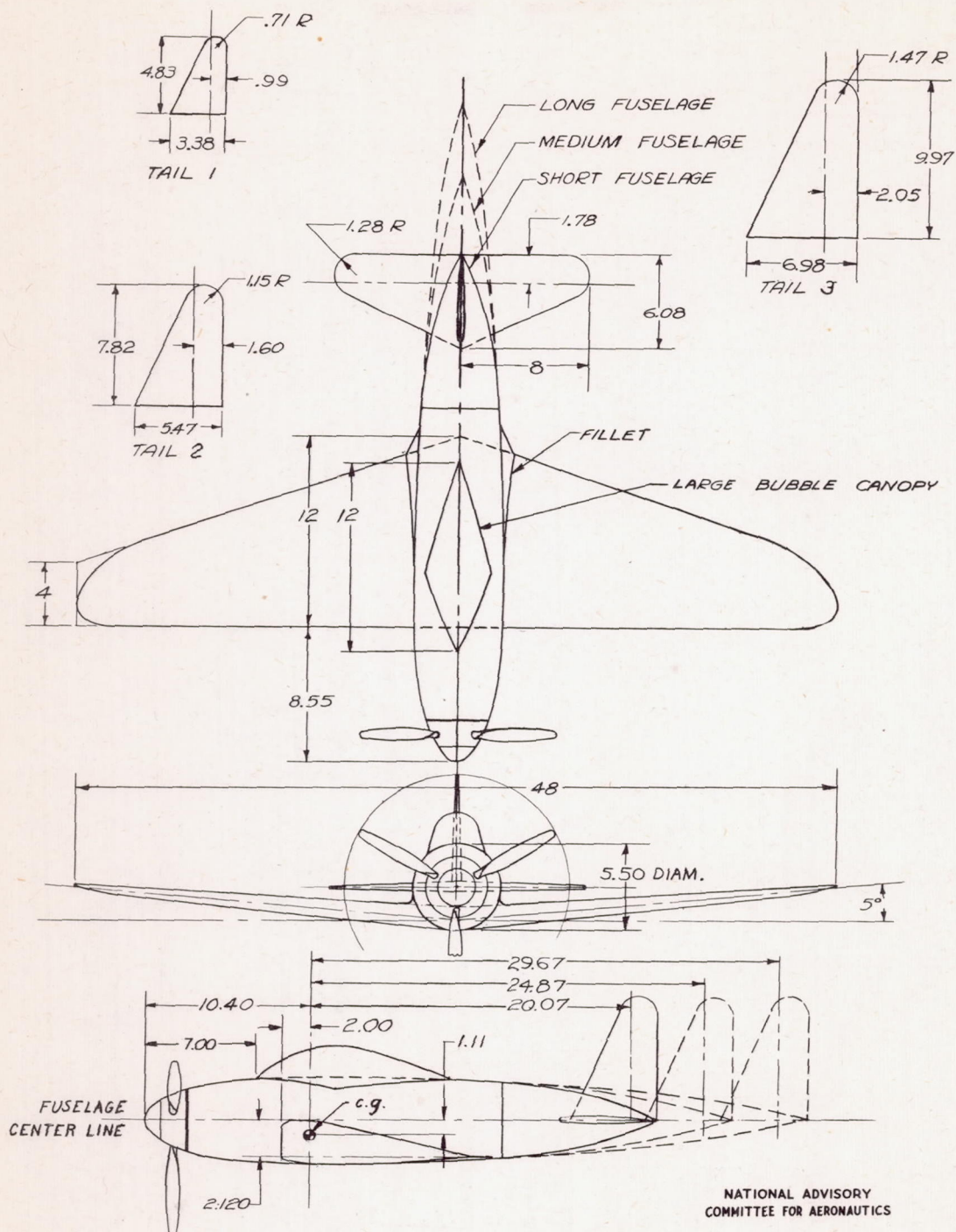


(d) Large box canopy.
Figure 1.- Continued.



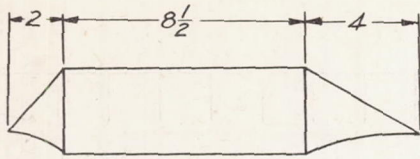
(e) Large bubble canopy open.

Figure 1.- Concluded.

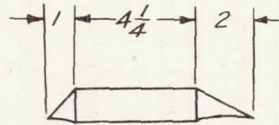


NATIONAL ADVISORY
COMMITTEE FOR AERONAUTICS

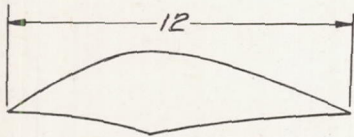
Figure 2.- Three-view drawing of model. Wing, NACA 23012 airfoil section; all rudder hinge lines located 29.3 percent of root chord from trailing edge of vertical tail; diameter of propeller, 14.25 inches; blade angle at 0.75 radius, 30°. (All dimensions in in.)



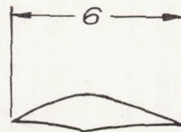
Large box canopy



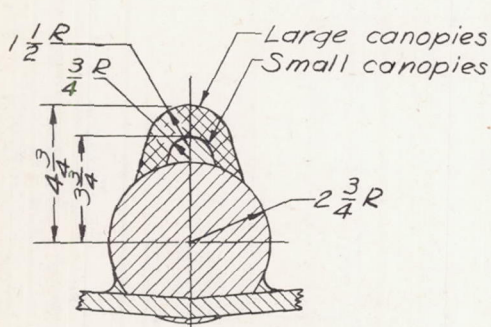
Small box canopy



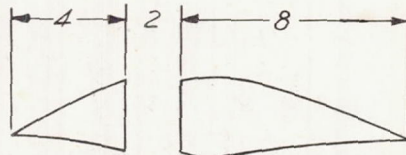
Large bubble canopy



Small bubble canopy

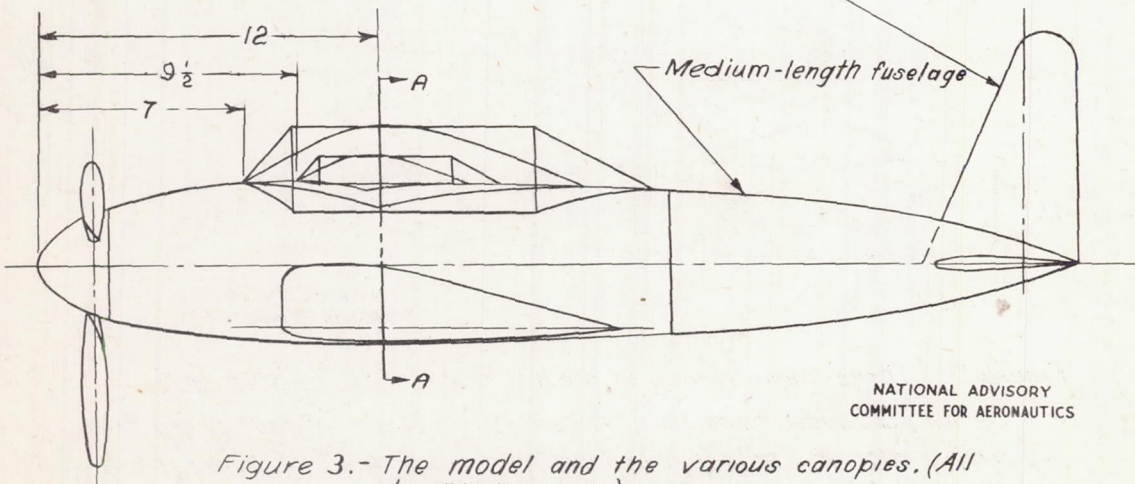


Section A-A



Large bubble canopy (open)

Vertical tail 2



NATIONAL ADVISORY
COMMITTEE FOR AERONAUTICS

Figure 3.- The model and the various canopies. (All dimensions in in.)

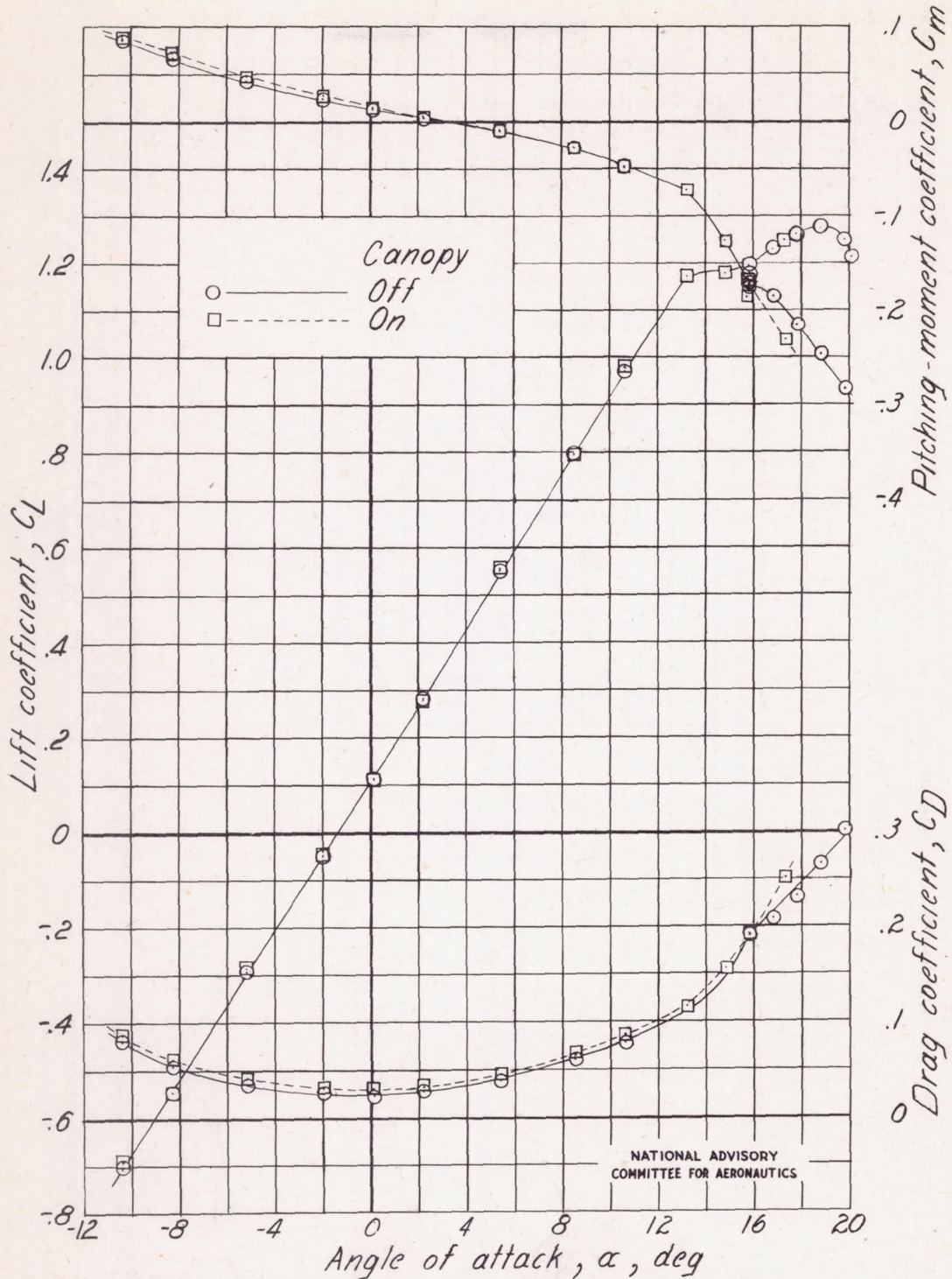
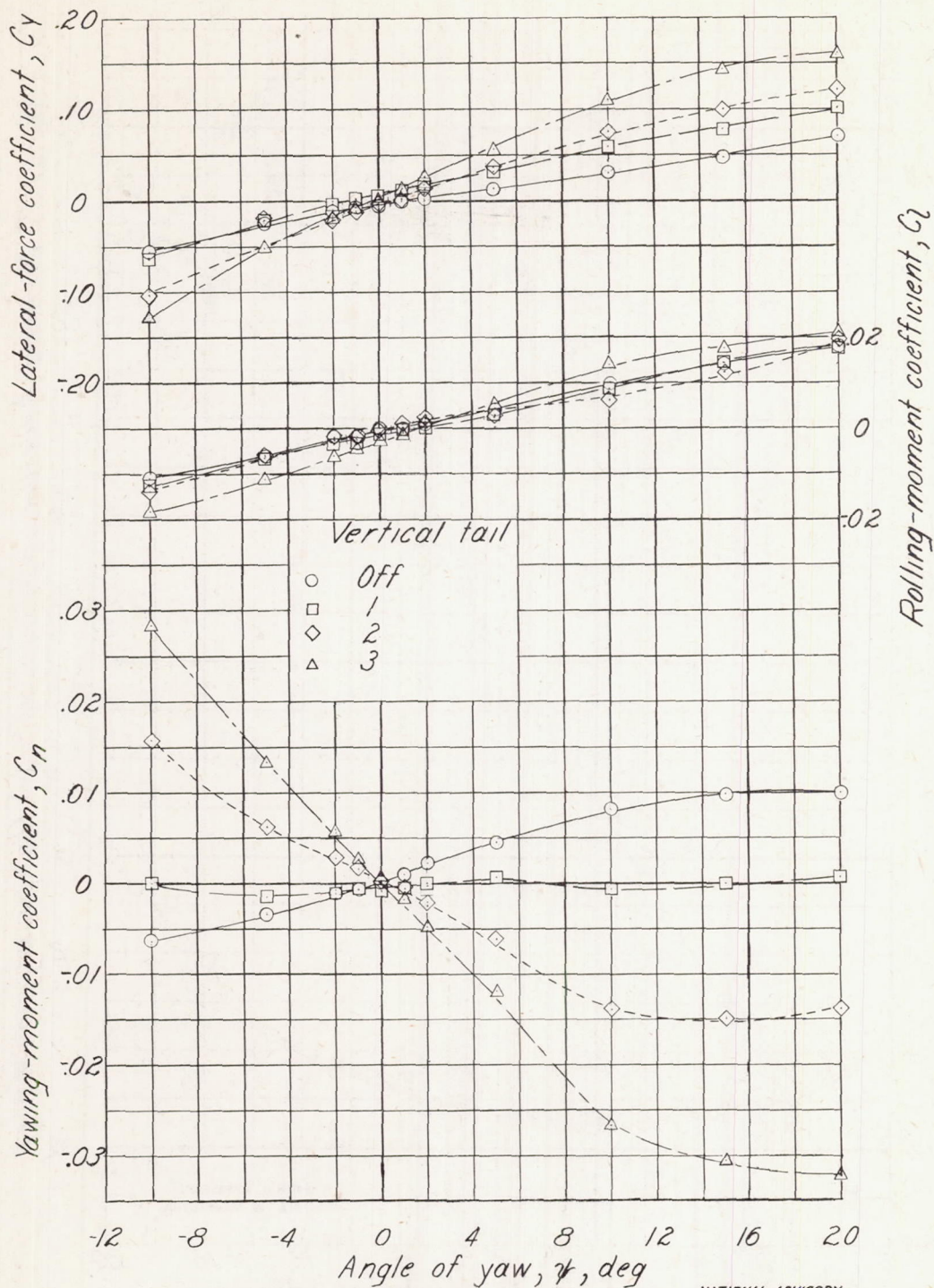


Figure 4.- Variation of lift, drag, and pitching-moment coefficients with angle of attack for model with and without large box canopy. Medium-length fuselage; vertical tail 2; $\psi = 0^\circ$.

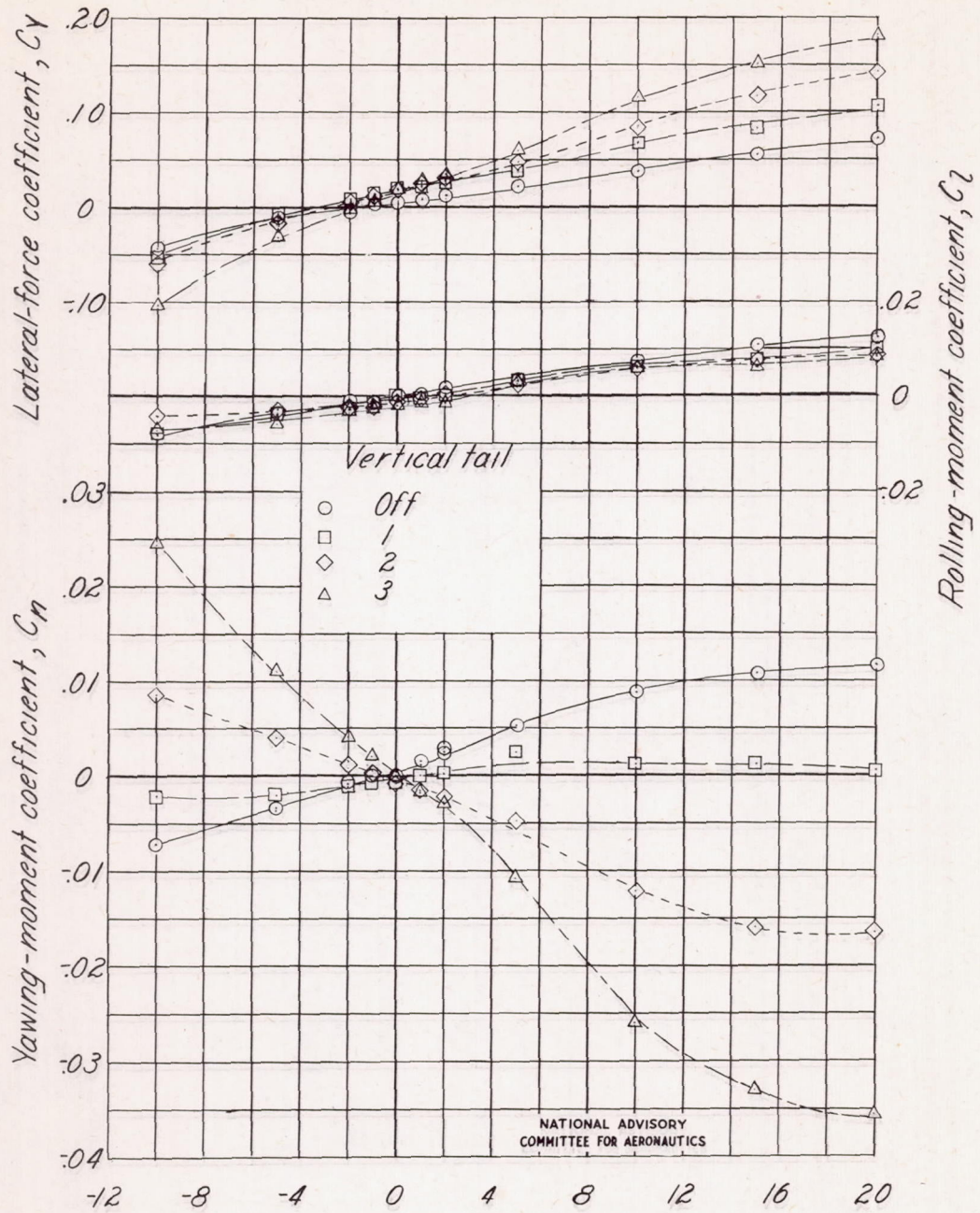
NATIONAL ADVISORY
COMMITTEE FOR AERONAUTICS



(a) Canopy off; $\alpha = 0.1^\circ$.

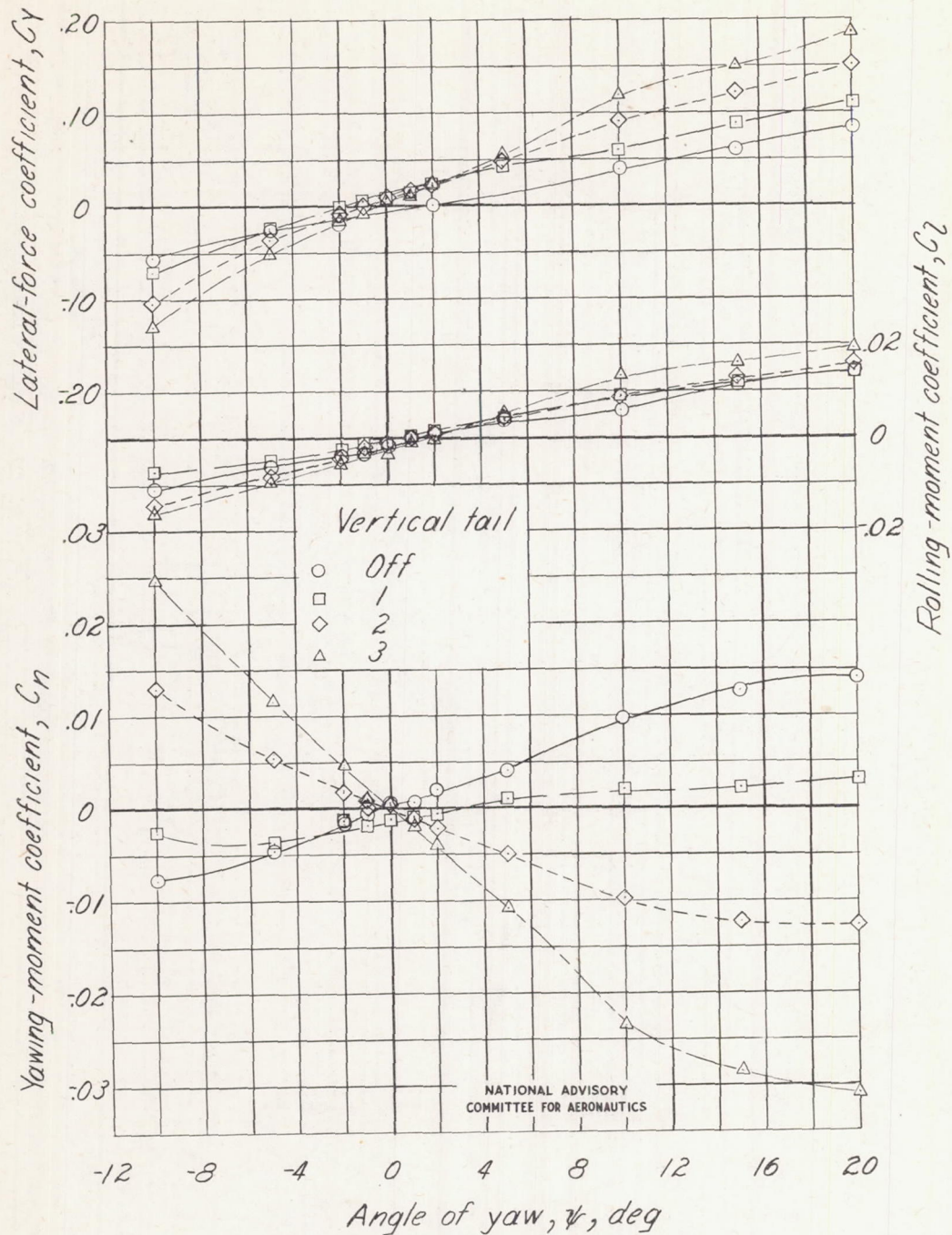
NATIONAL ADVISORY
COMMITTEE FOR AERONAUTICS

Figure 5.-Effect of vertical-tail area on variation of yawing-moment, rolling-moment, and lateral-force coefficients with angle of yaw. Medium-length fuselage.



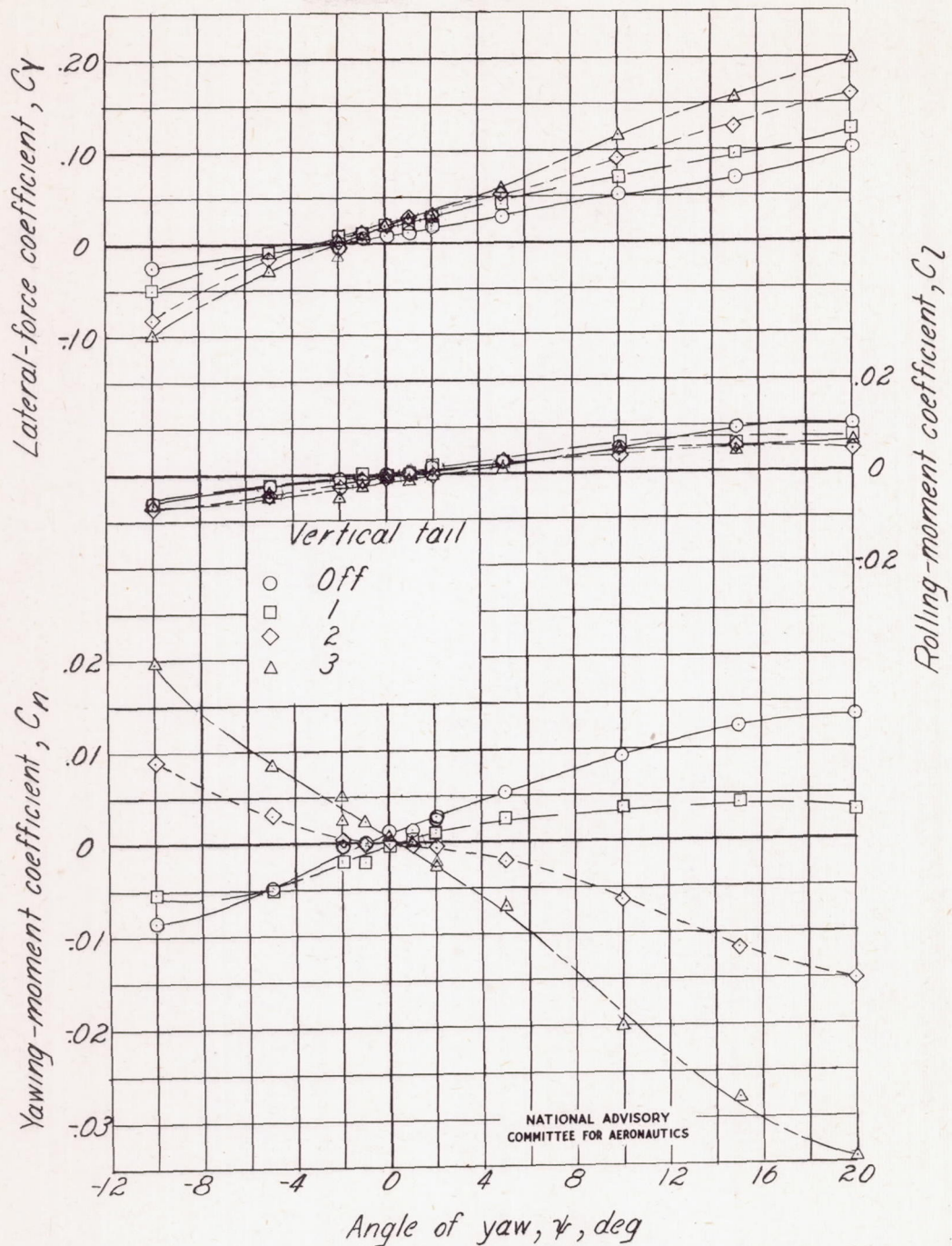
Angle of yaw, ψ , deg
 (b) Canopy off ; $\alpha = 10.6^\circ$
 Figure 5.-Continued.

NATIONAL ADVISORY
 COMMITTEE FOR AERONAUTICS



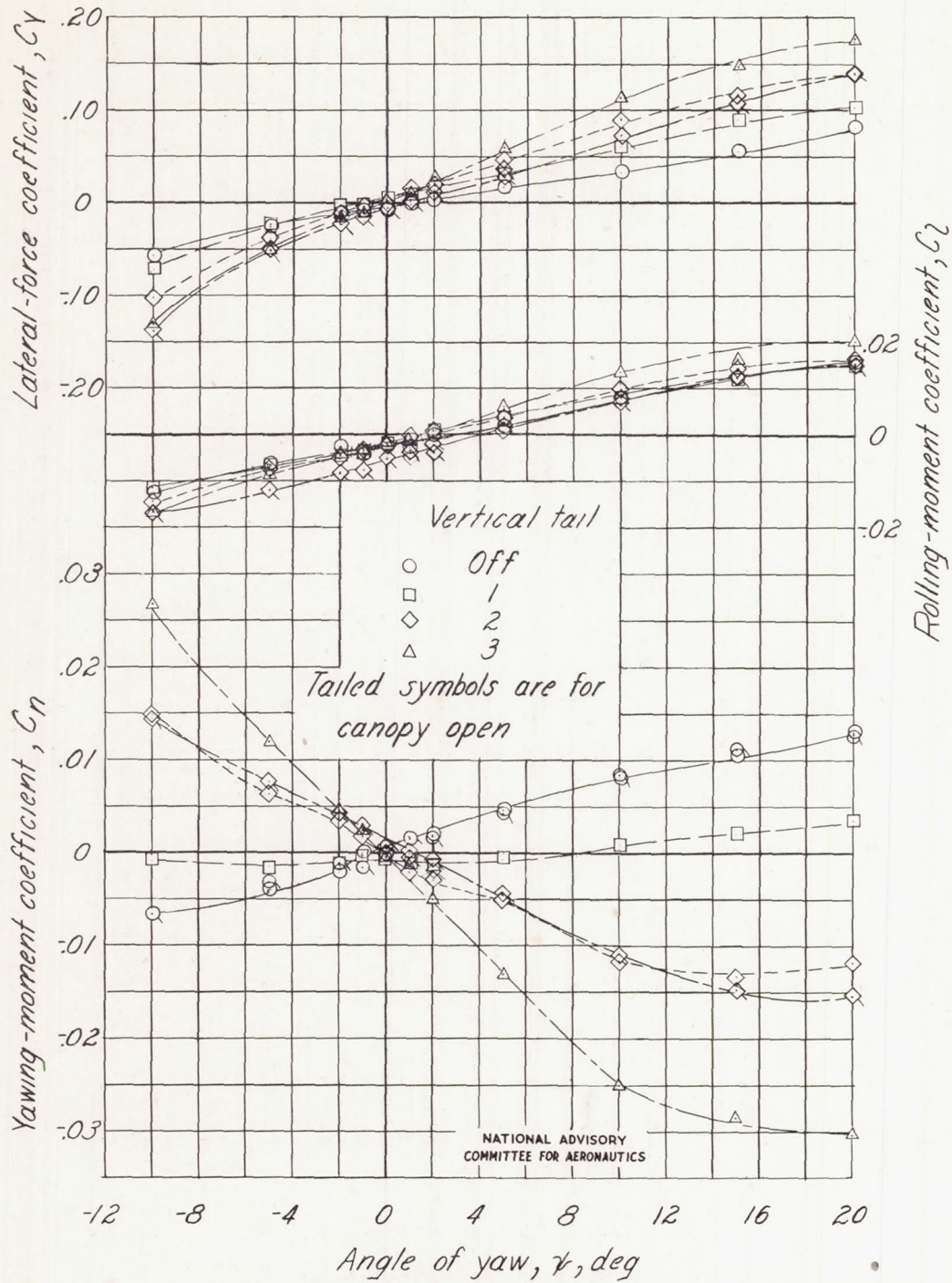
(c) Large box canopy; $\alpha = 0.1^\circ$.

Figure 5.-Continued.



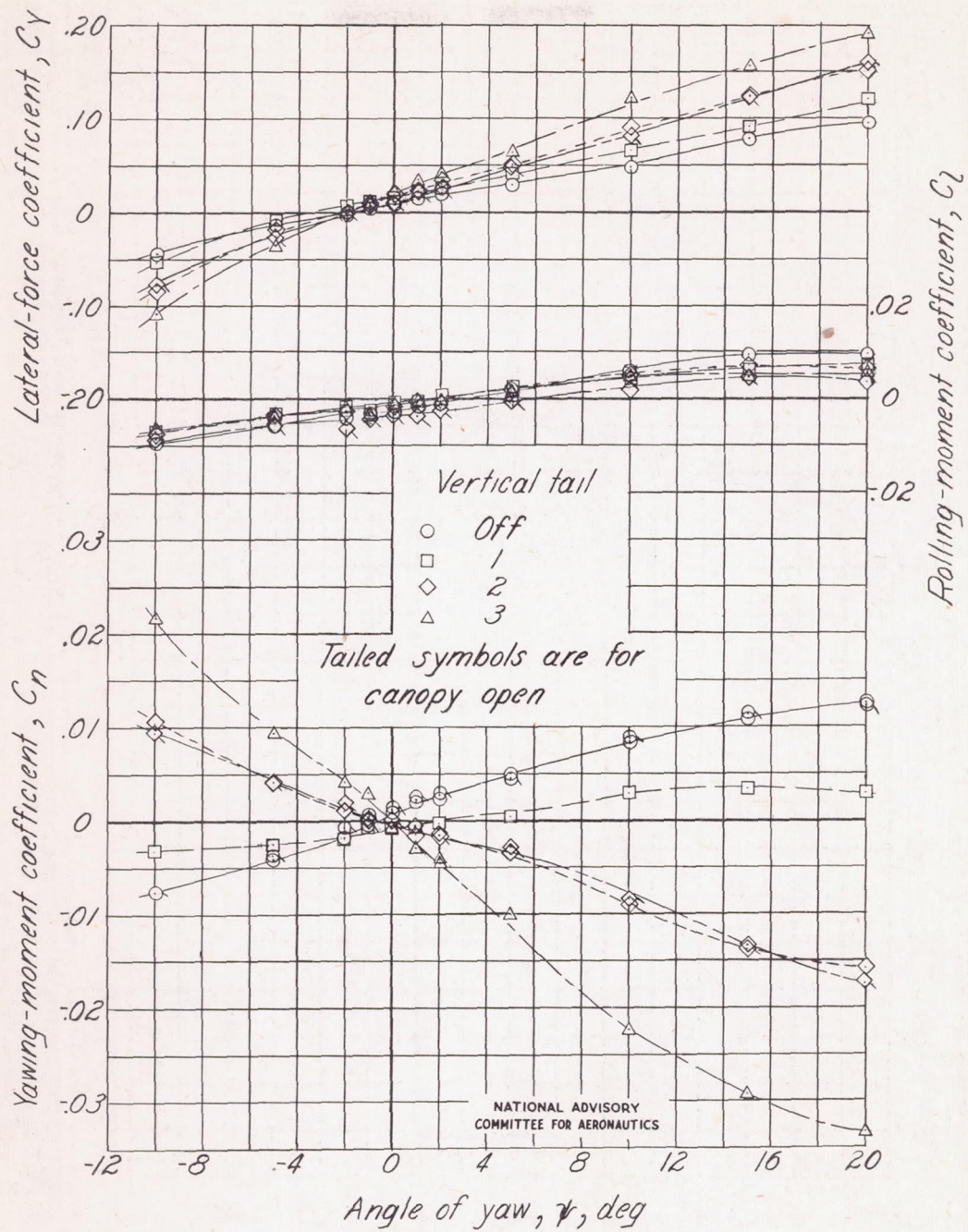
(d) Large box canopy ; $\alpha = 10.6^\circ$.

Figure 5.-Continued.



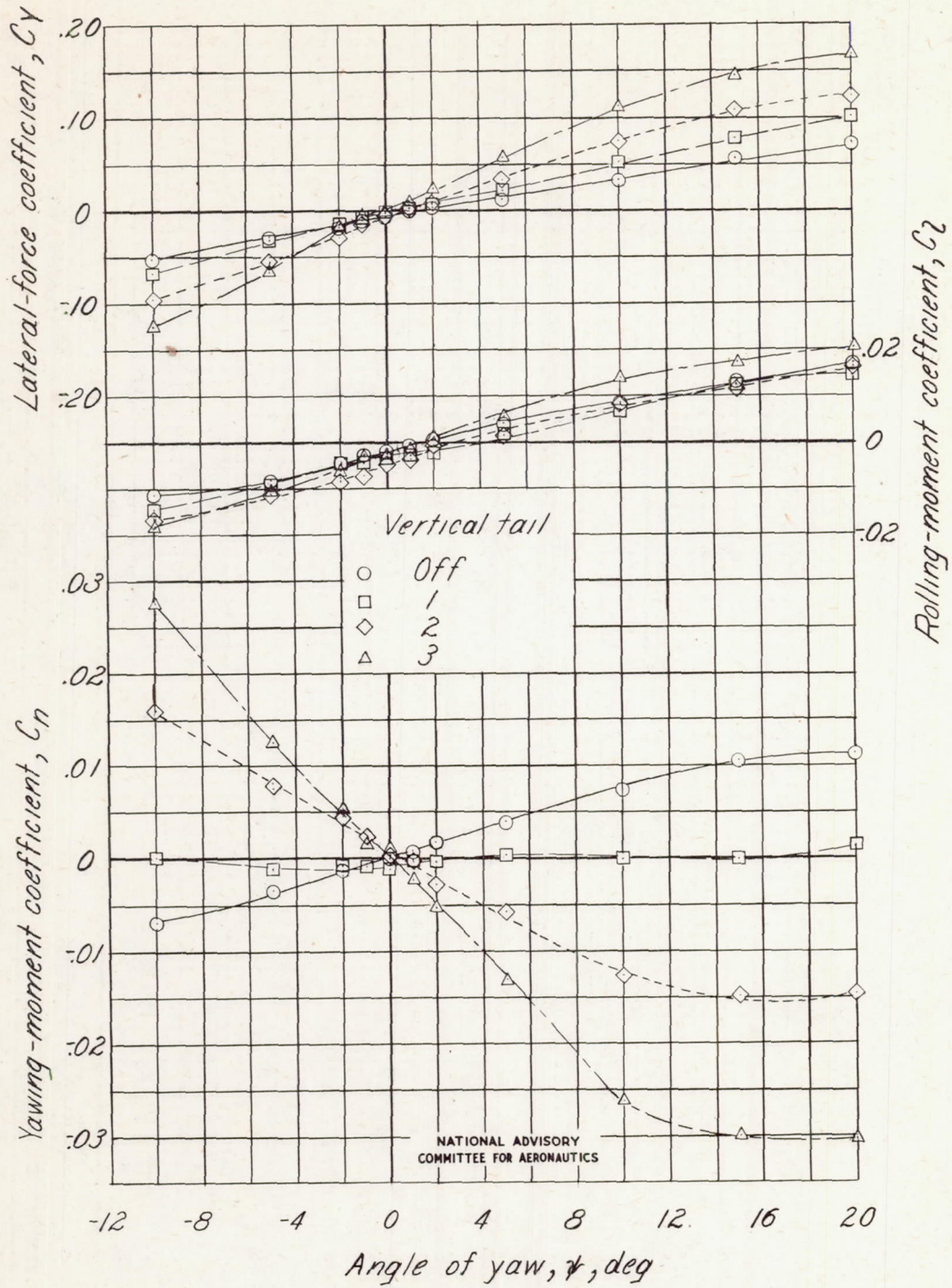
(e) Large bubble canopy; $\alpha = 0.1^\circ$.
Figure 5.-Continued.

NATIONAL ADVISORY
COMMITTEE FOR AERONAUTICS



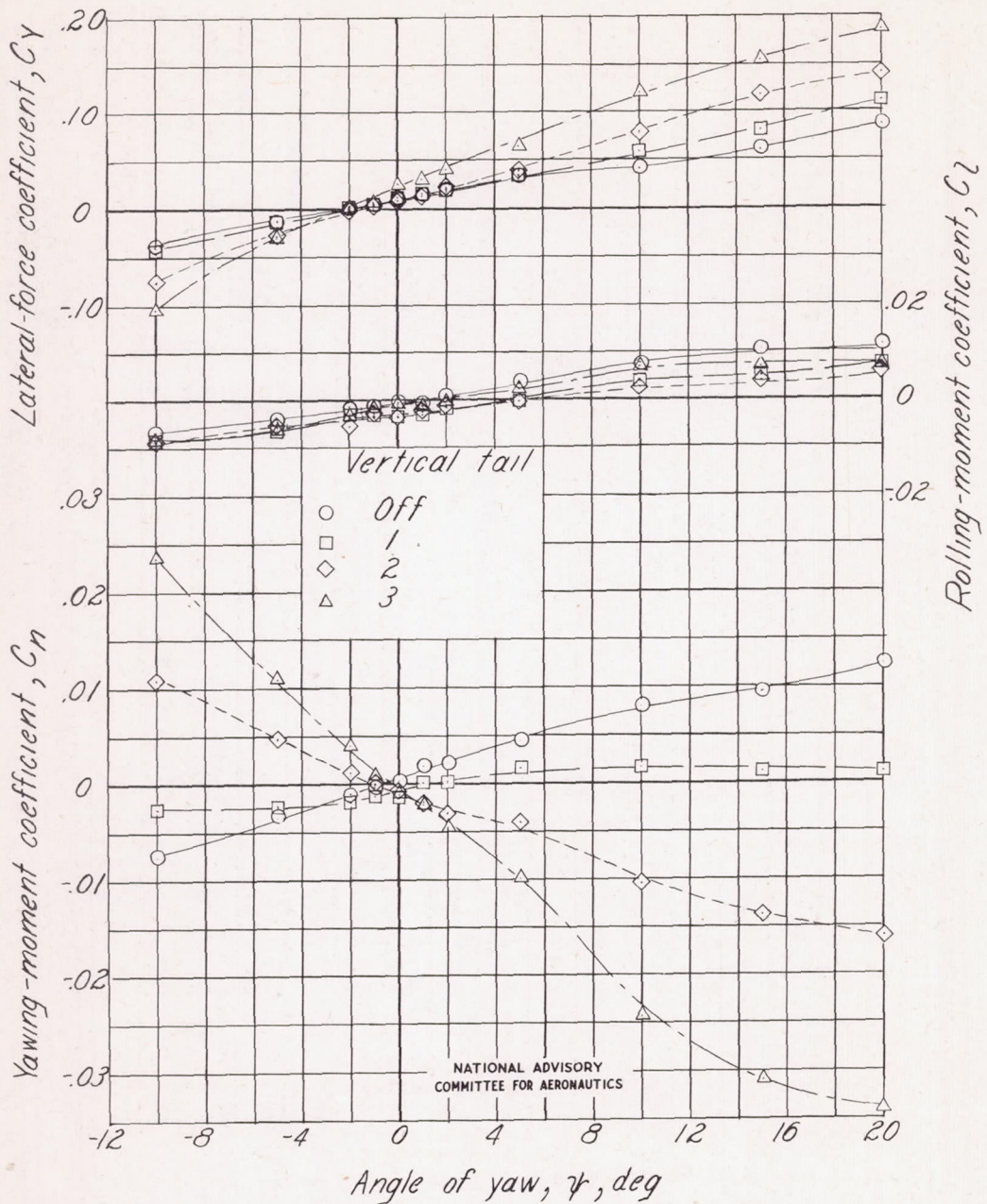
(f) Large bubble canopy; $\alpha = 10.6^\circ$.

Figure 5.- Continued.

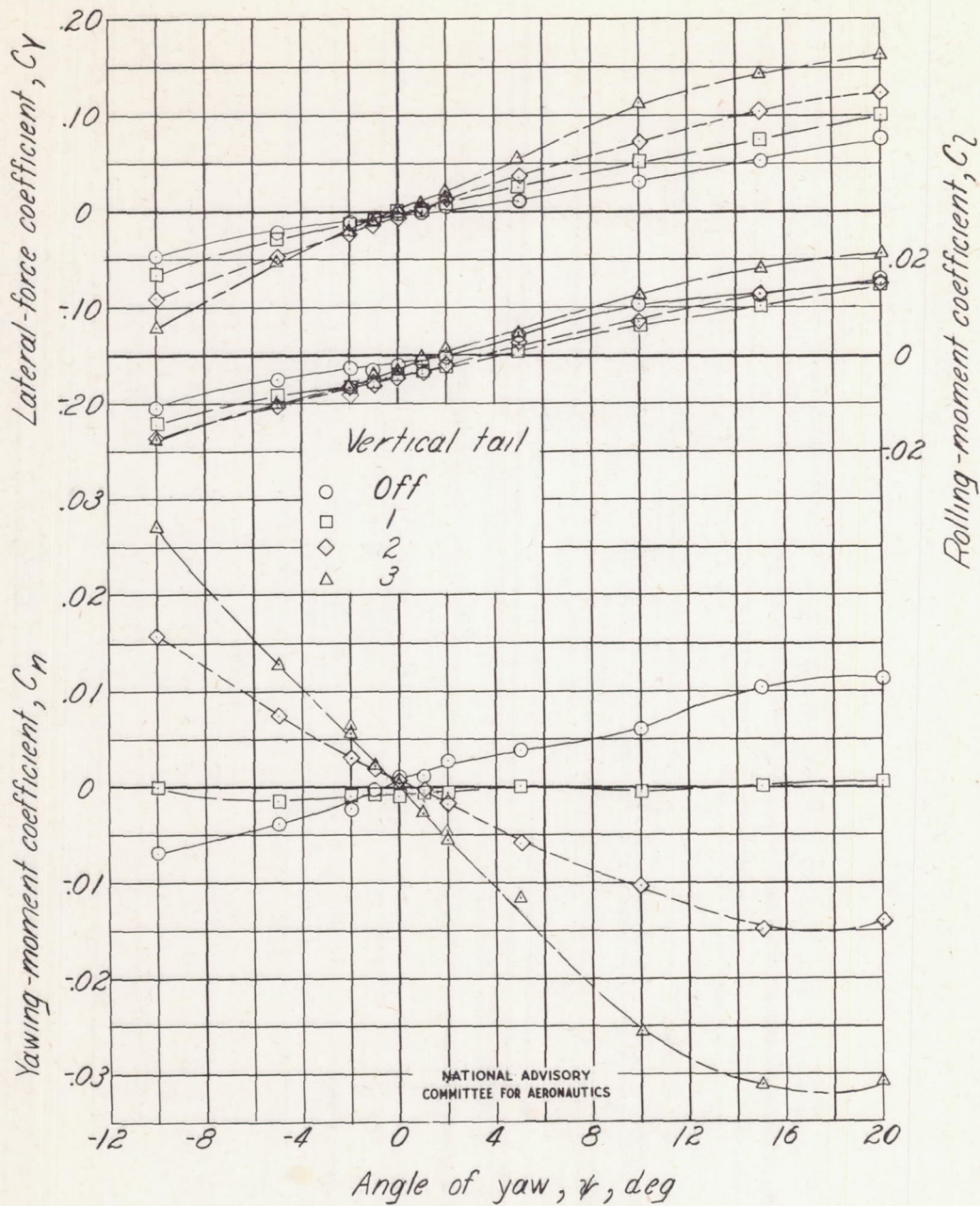


NATIONAL ADVISORY
COMMITTEE FOR AERONAUTICS

(g) Small box canopy ; $\alpha = 0.1^\circ$.
Figure 5.-Continued.

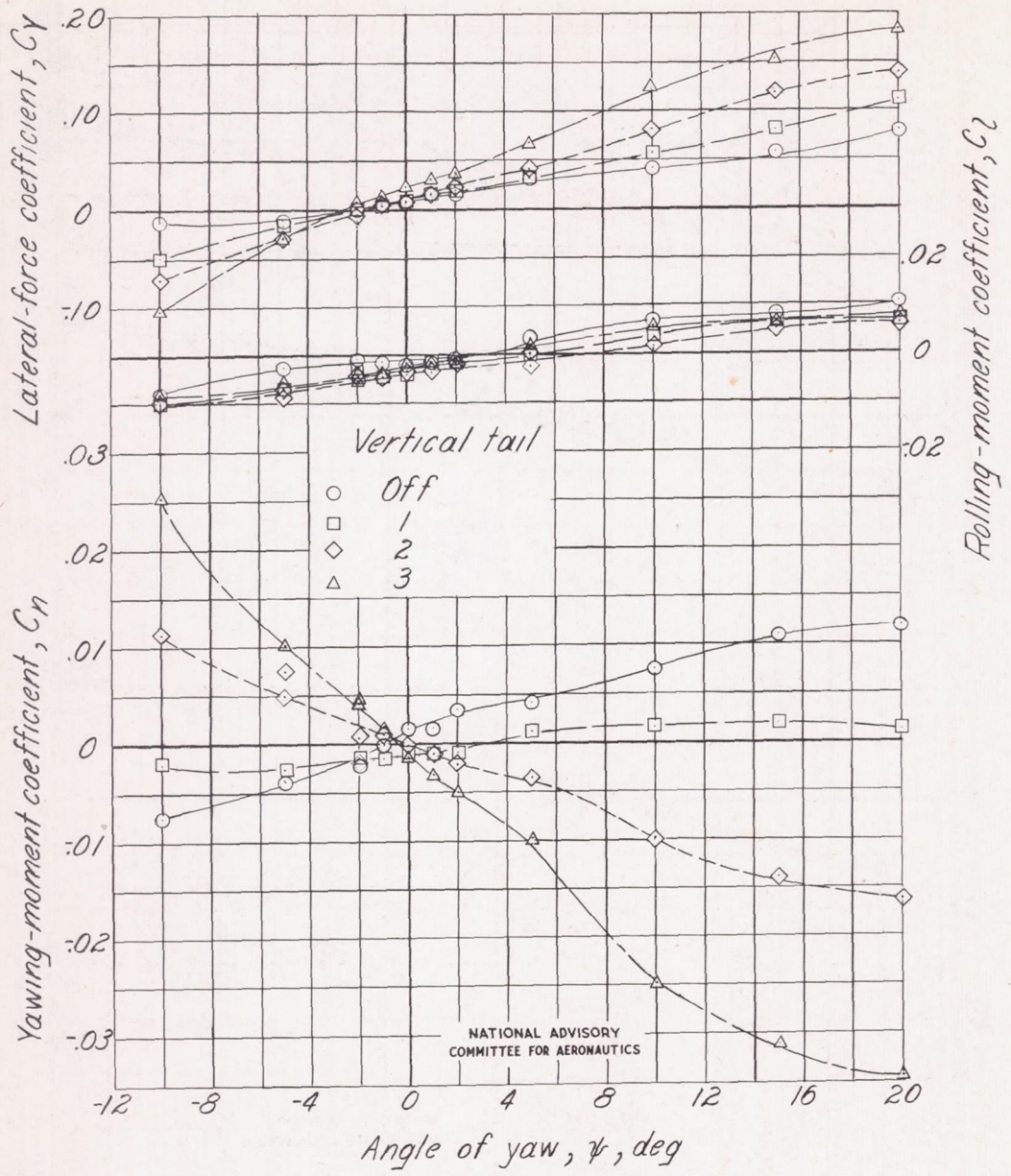


Angle of yaw, ψ , deg
 (h) Small box canopy ; $\alpha = 10.6^\circ$
 Figure 5.-Continued.

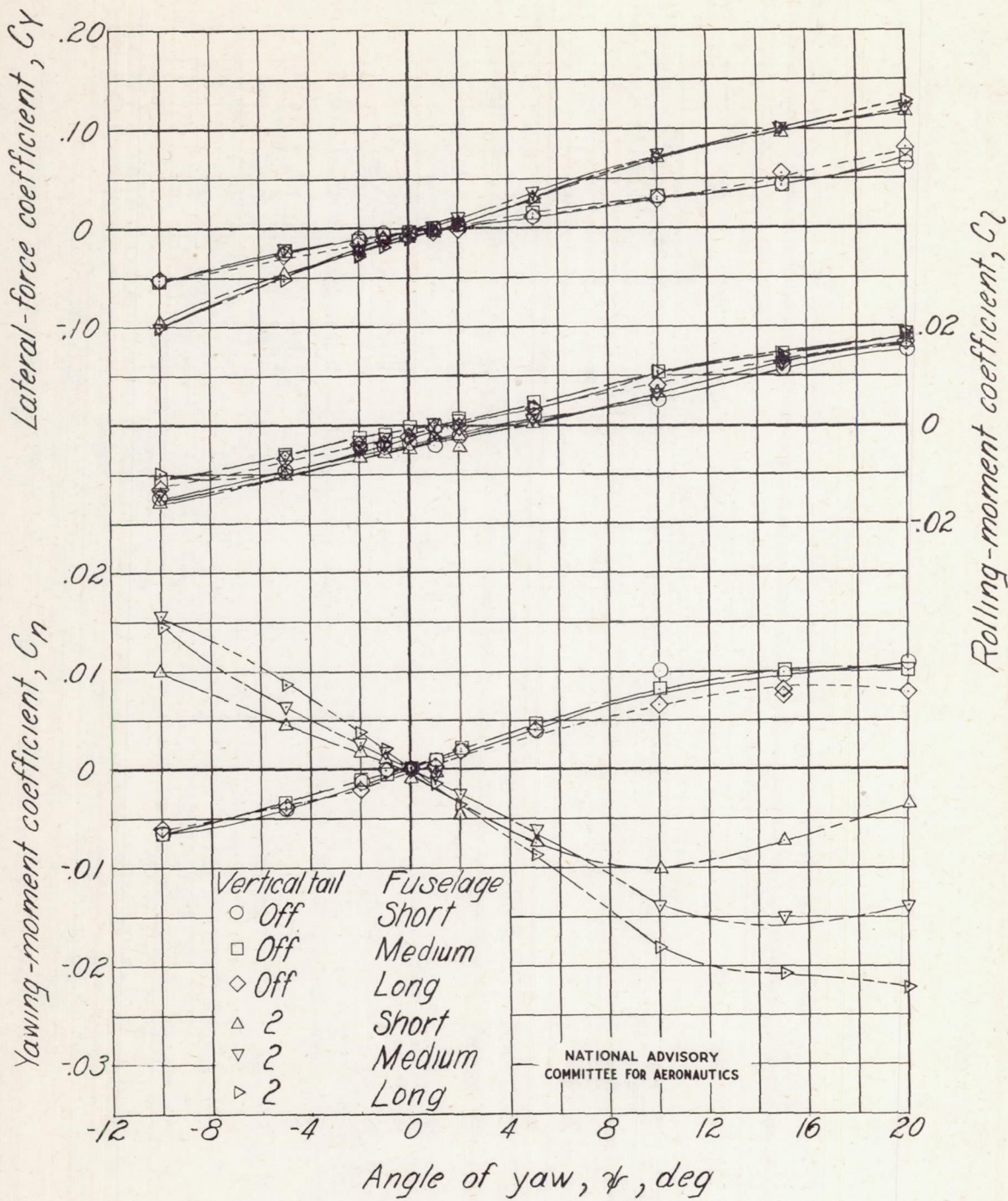


NATIONAL ADVISORY
COMMITTEE FOR AERONAUTICS

Angle of yaw, ψ , deg
(1) Small bubble canopy, $\alpha = 0.1^\circ$.
Figure 5.-Continued.

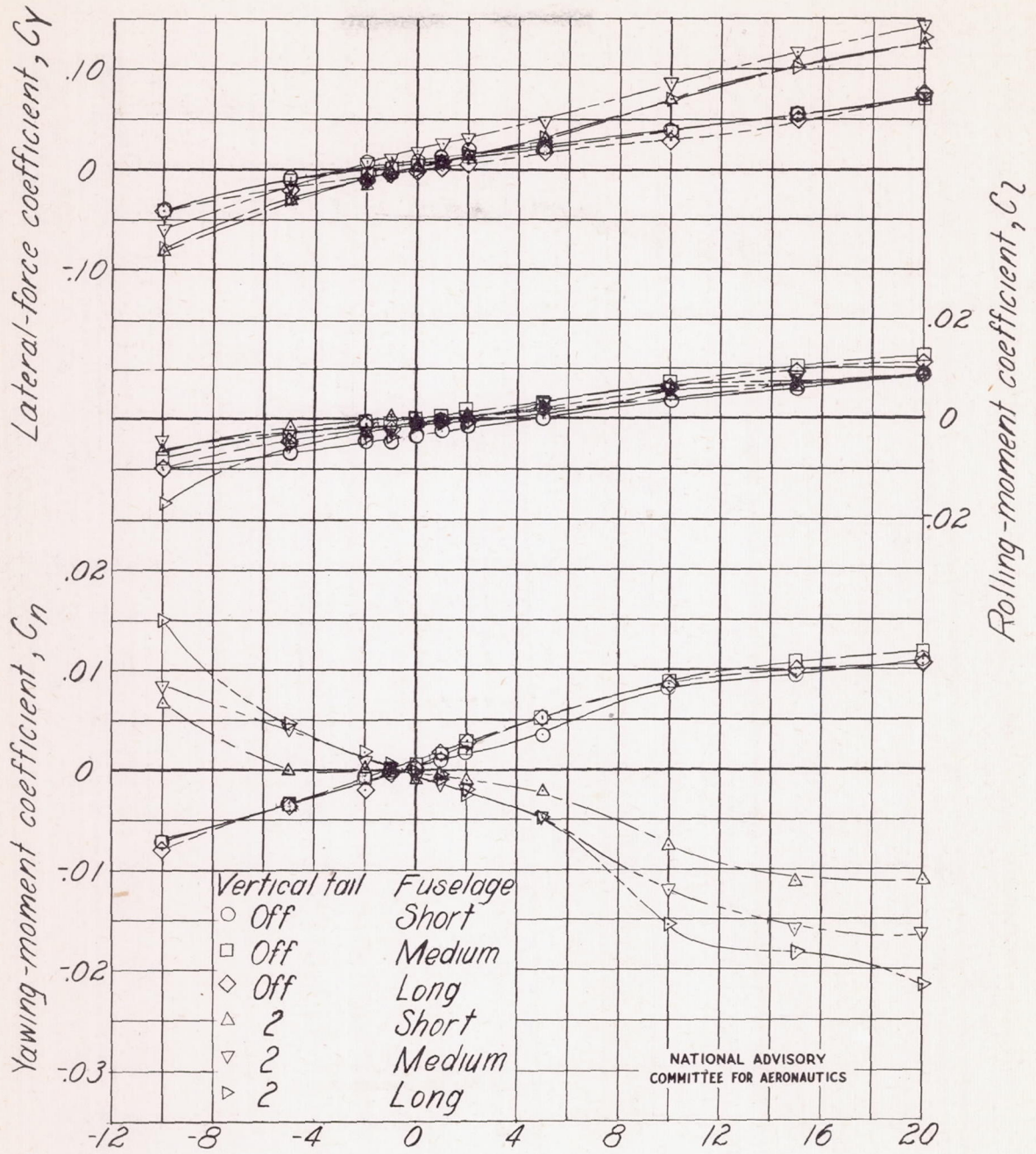


(J) Small bubble canopy ; $\alpha = 10.6^\circ$.
 Figure 5.-Concluded.



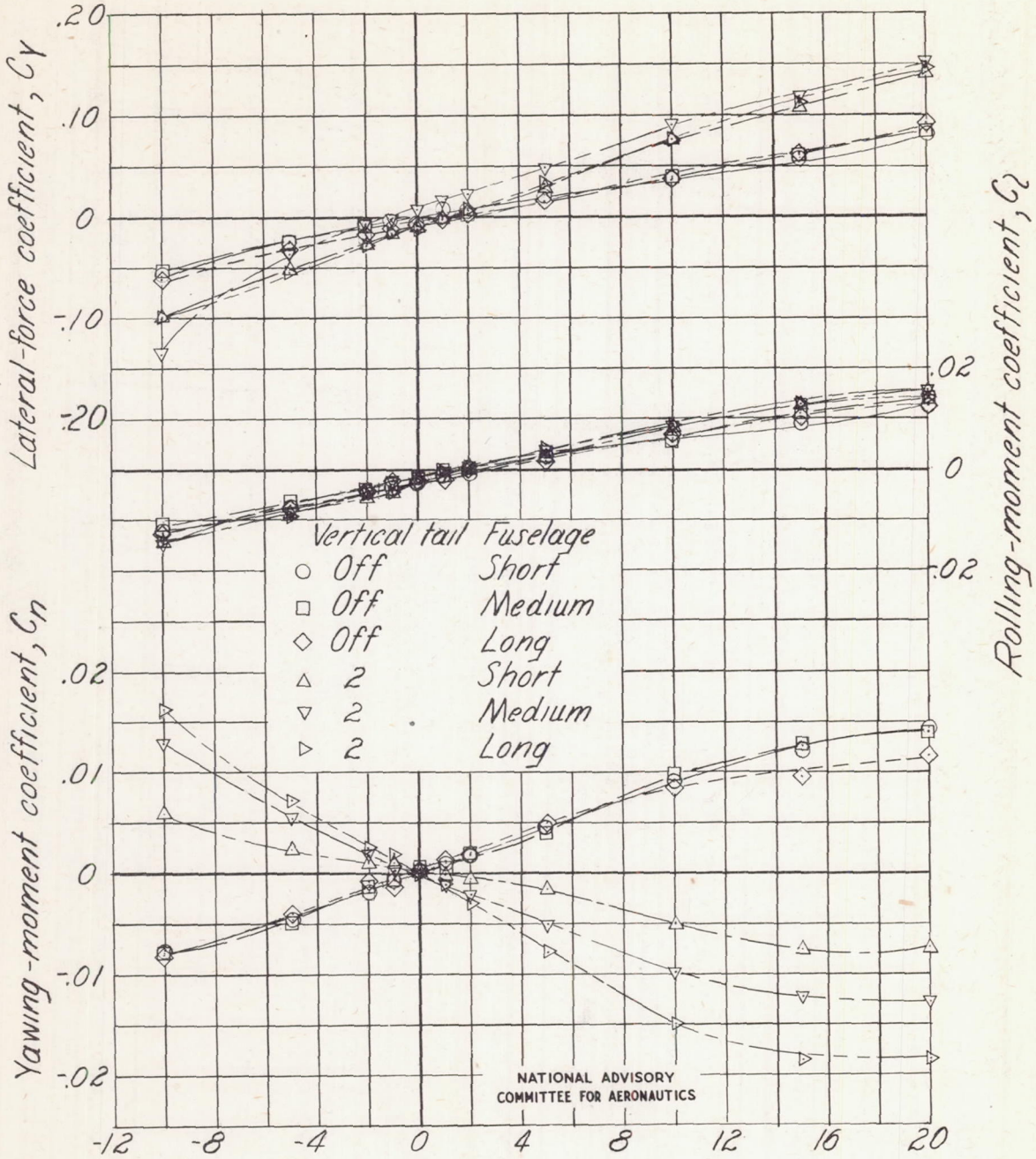
(a) Canopy off; $\alpha = 0.1^\circ$.

Figure 6.-Effect of fuselage length on variation of yawing-moment, rolling-moment, and lateral-force coefficients with angle of yaw.

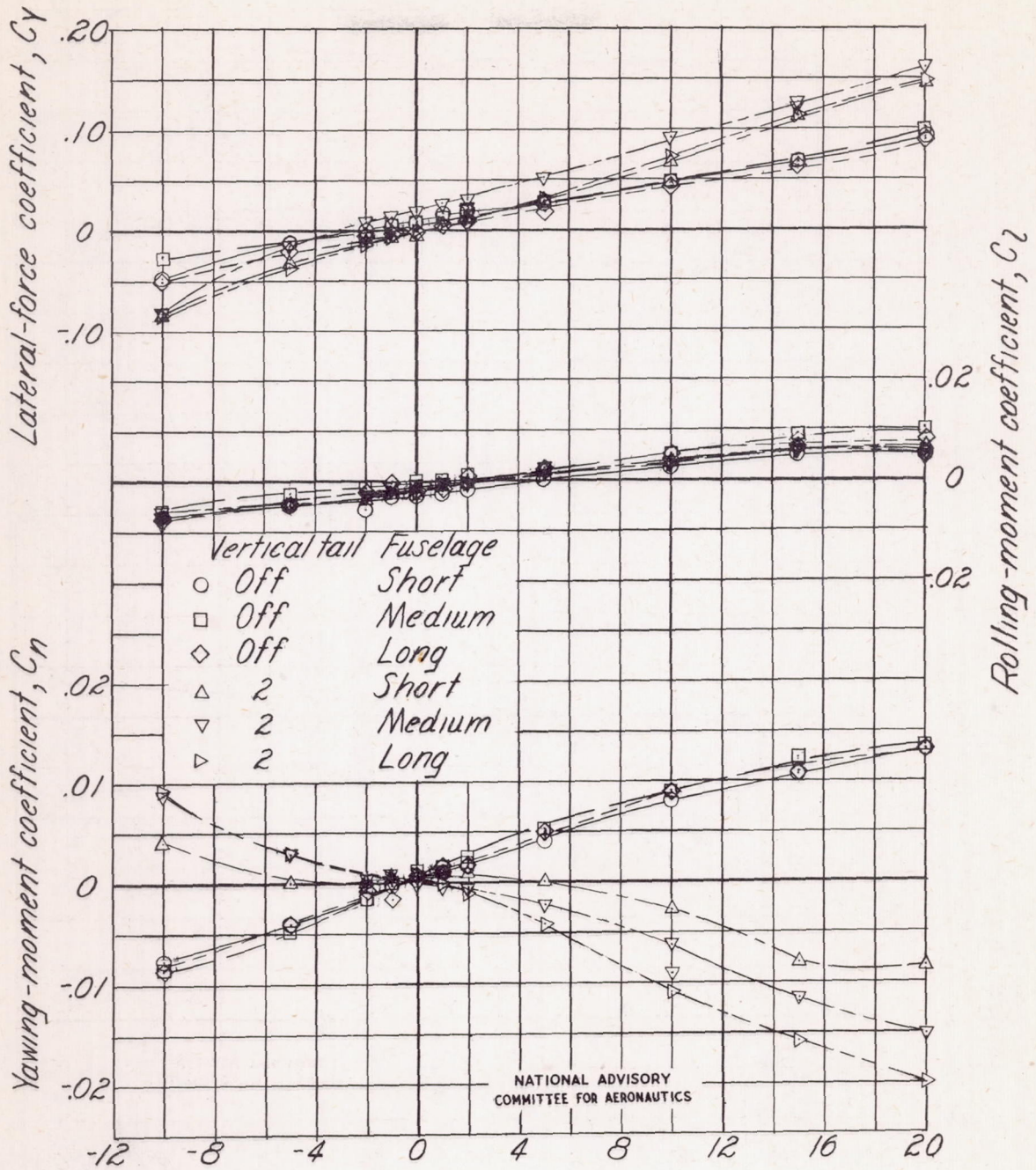


NATIONAL ADVISORY COMMITTEE FOR AERONAUTICS

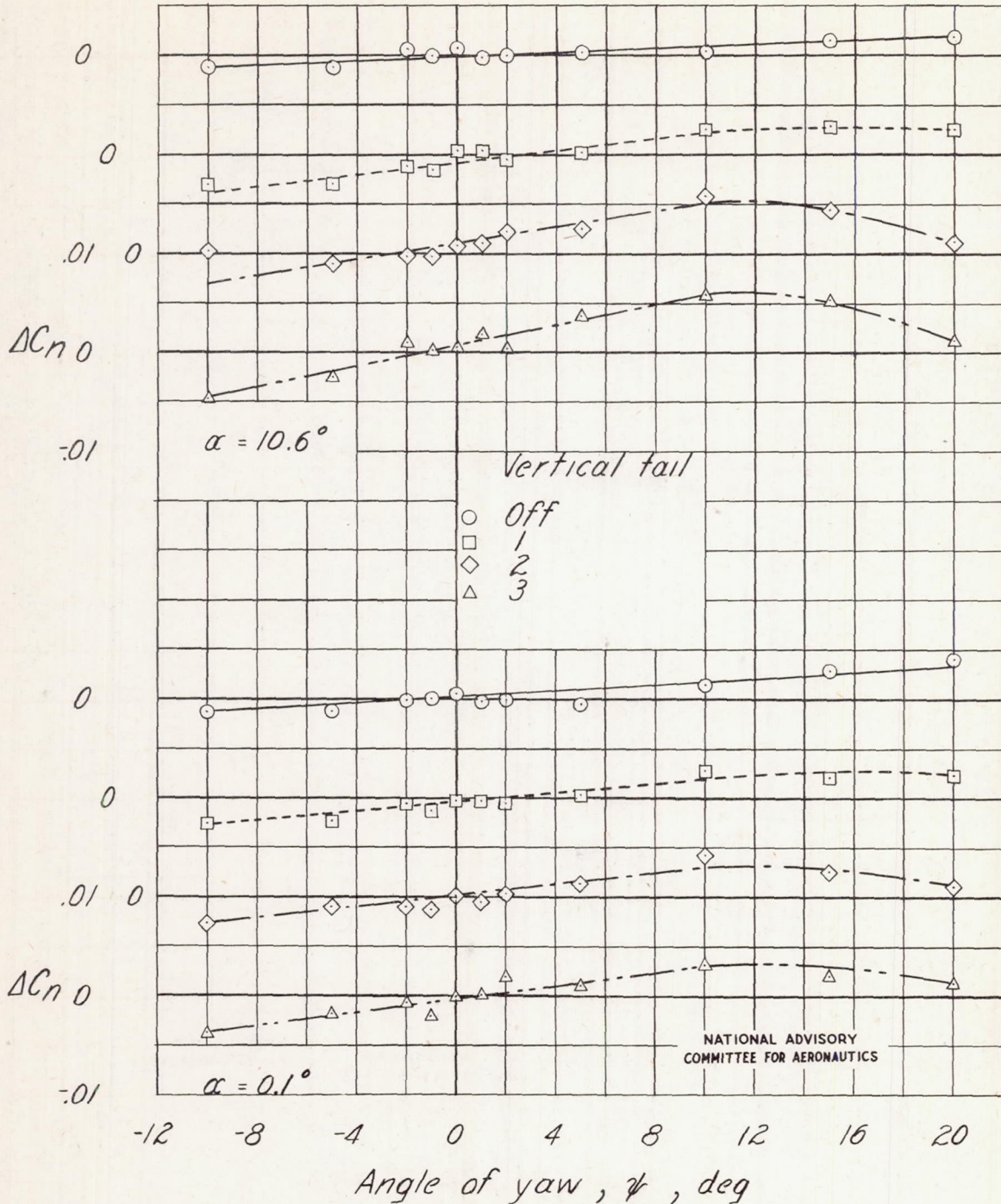
Angle of yaw, ψ , deg
 (b) Canopy off; $\alpha = 10.6^\circ$
 Figure 6.-Continued.



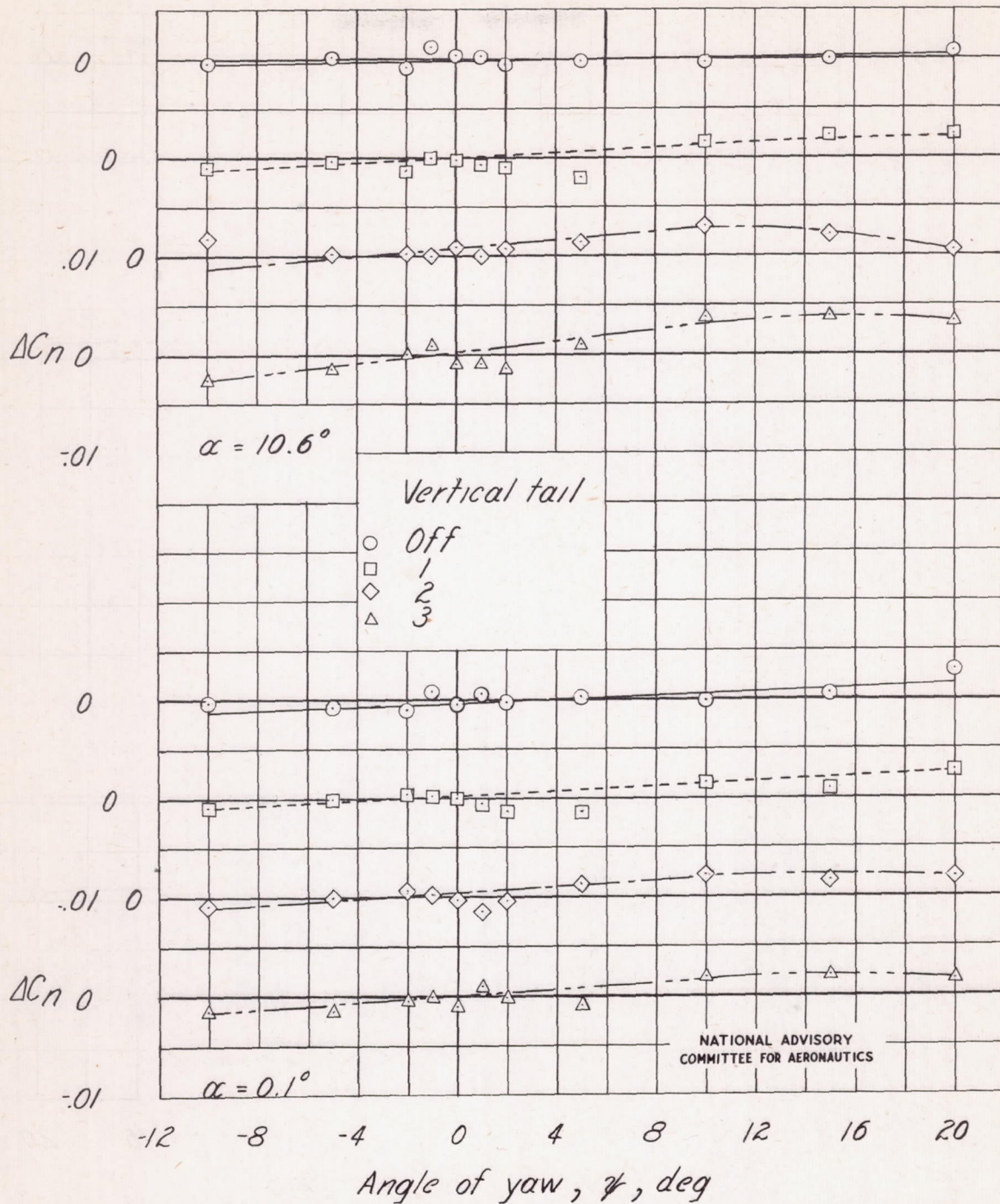
(c) Large box canopy ; $\alpha = 0.1^\circ$.
Figure 6.-Continued.



Angle of yaw, ψ , deg
 (d) Large box canopy ; $\alpha = 10.6^\circ$.
 Figure 6 .-Concluded.

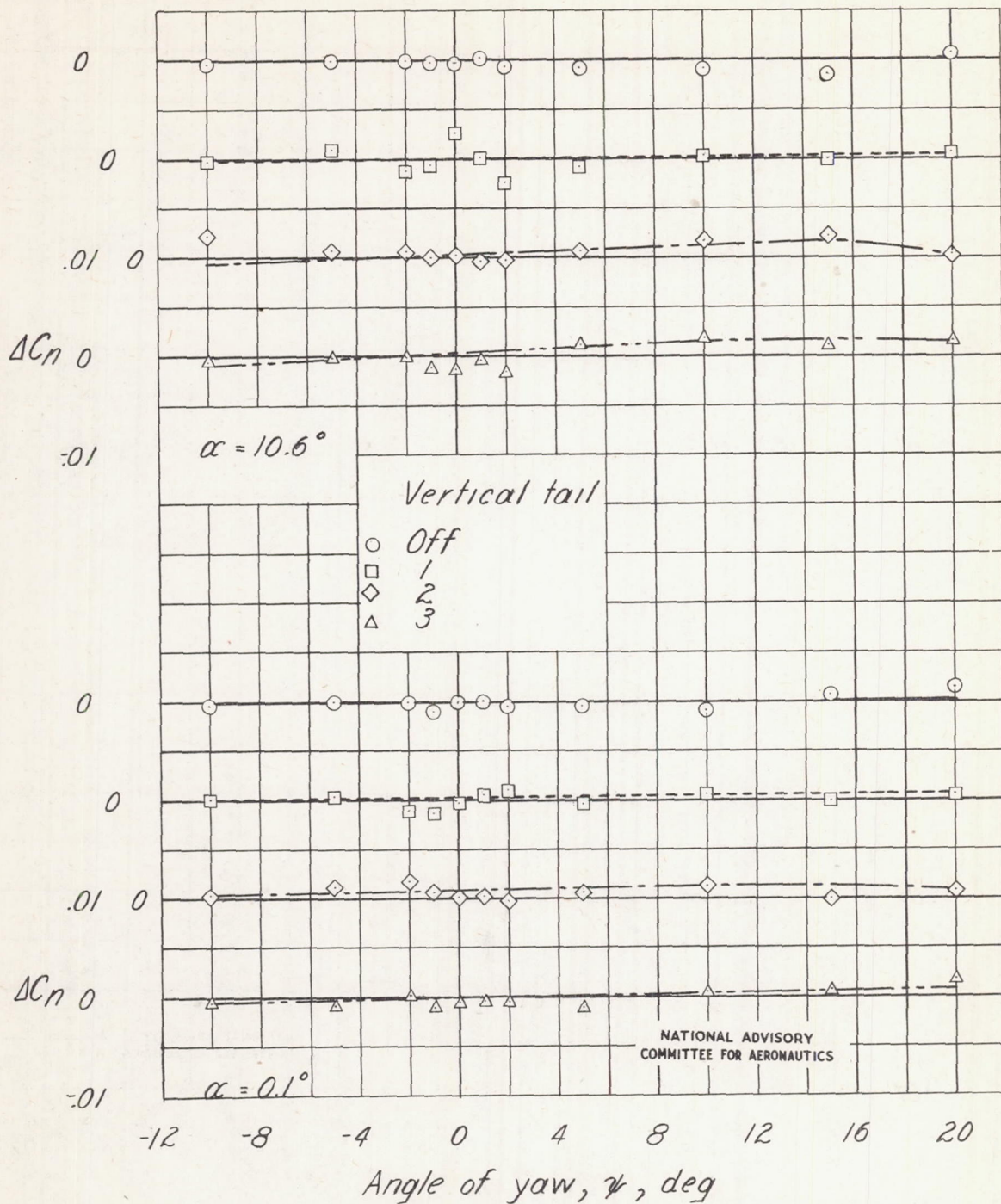


(a) Large box canopy ; medium-length fuselage.
 Figure 7.-Increment of C_n resulting from addition of canopy to model.



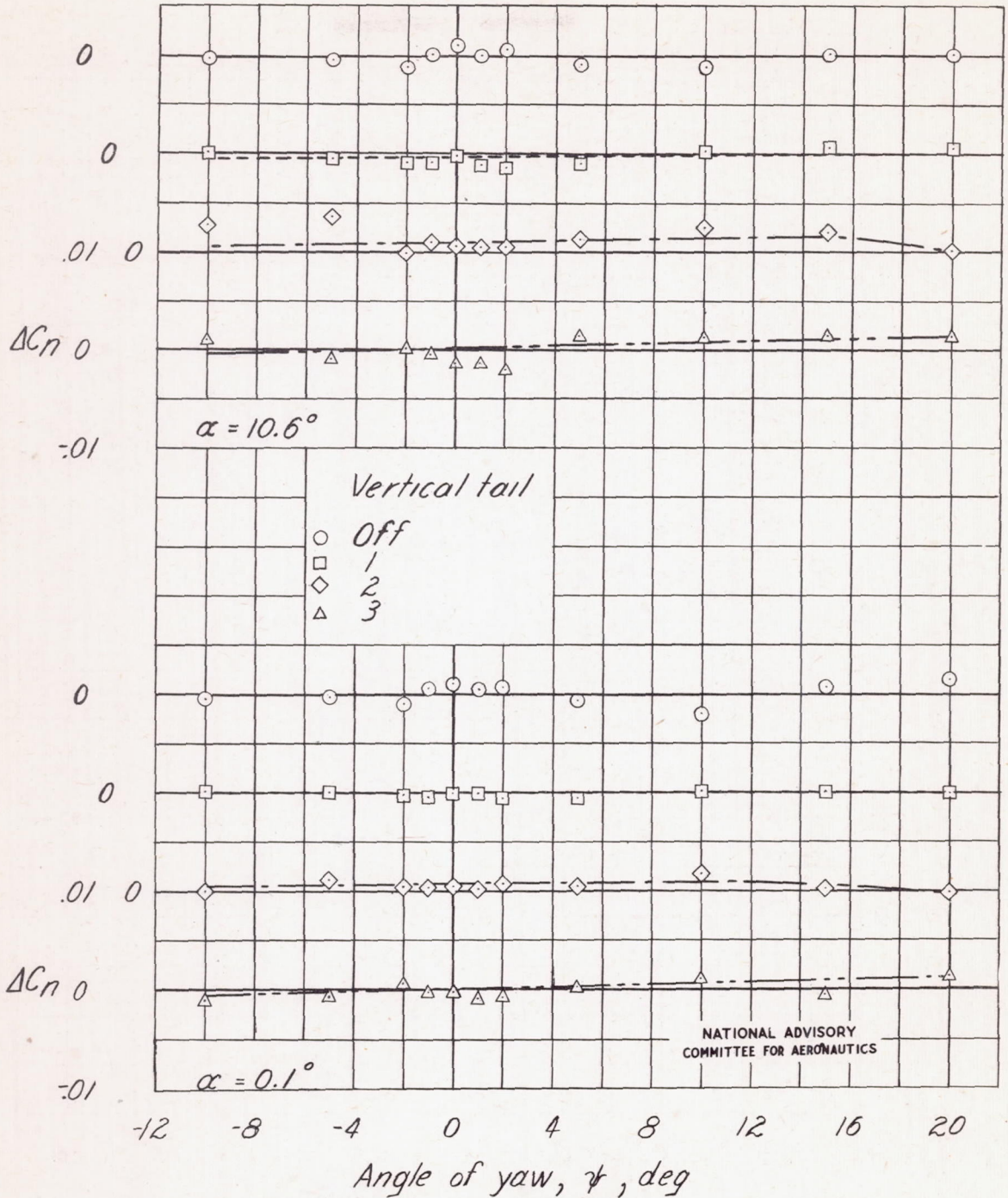
(b) Large bubble canopy; medium-length fuselage.

Figure 7.-Continued.

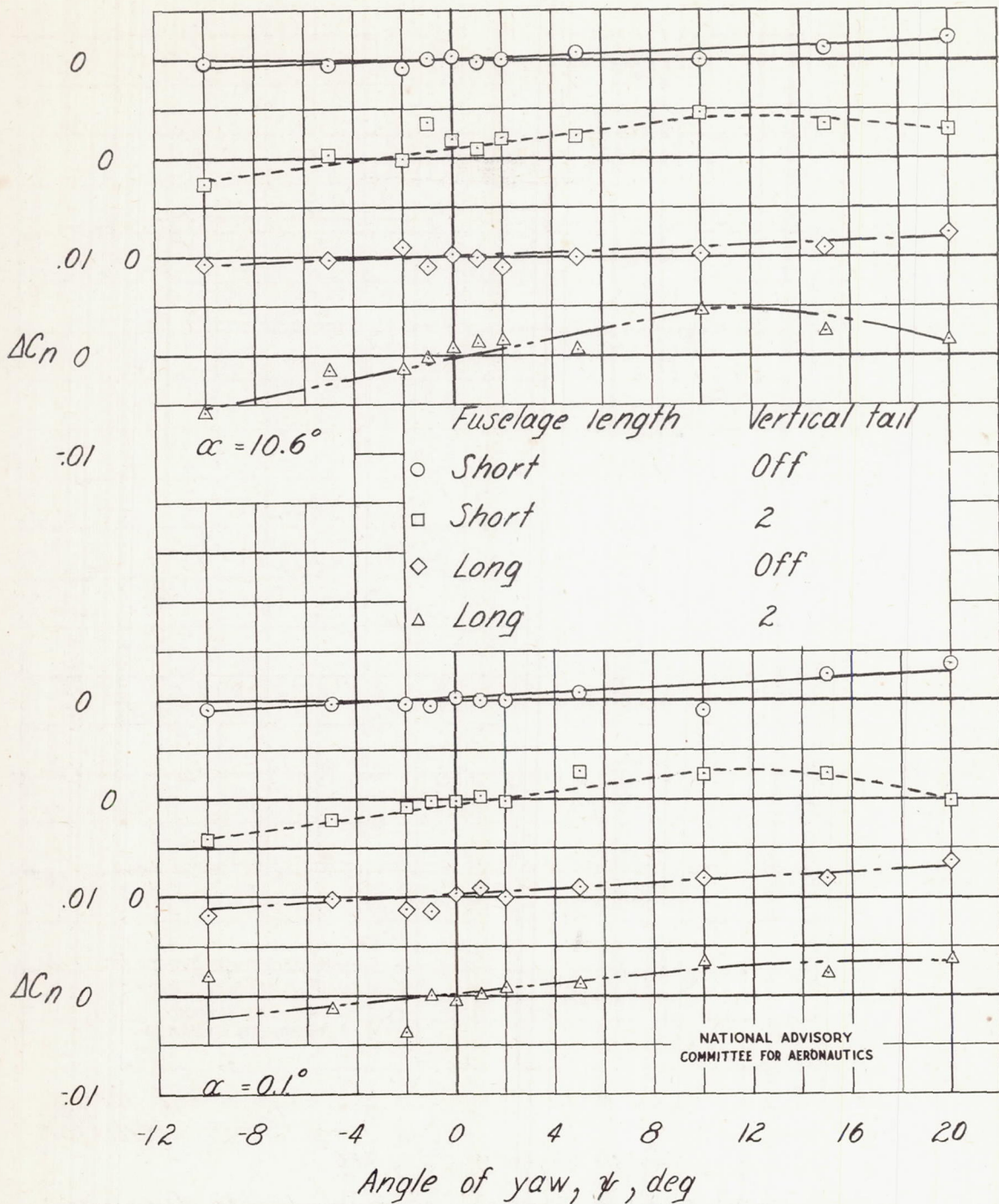


(c) Small box canopy ; medium-length fuselage.

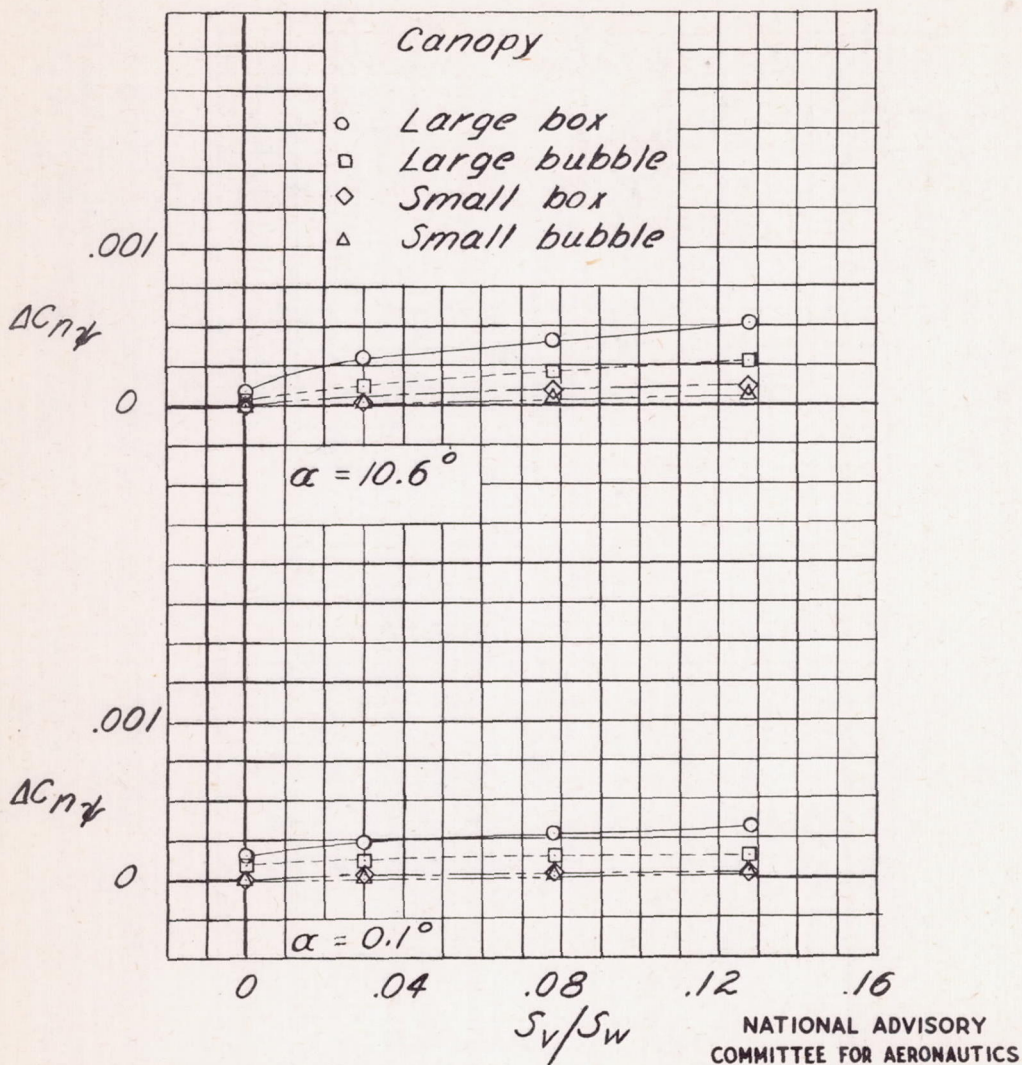
Figure 7.-Continued.



(d) Small bubble canopy ; medium-length fuselage.
Figure 7.-Continued.

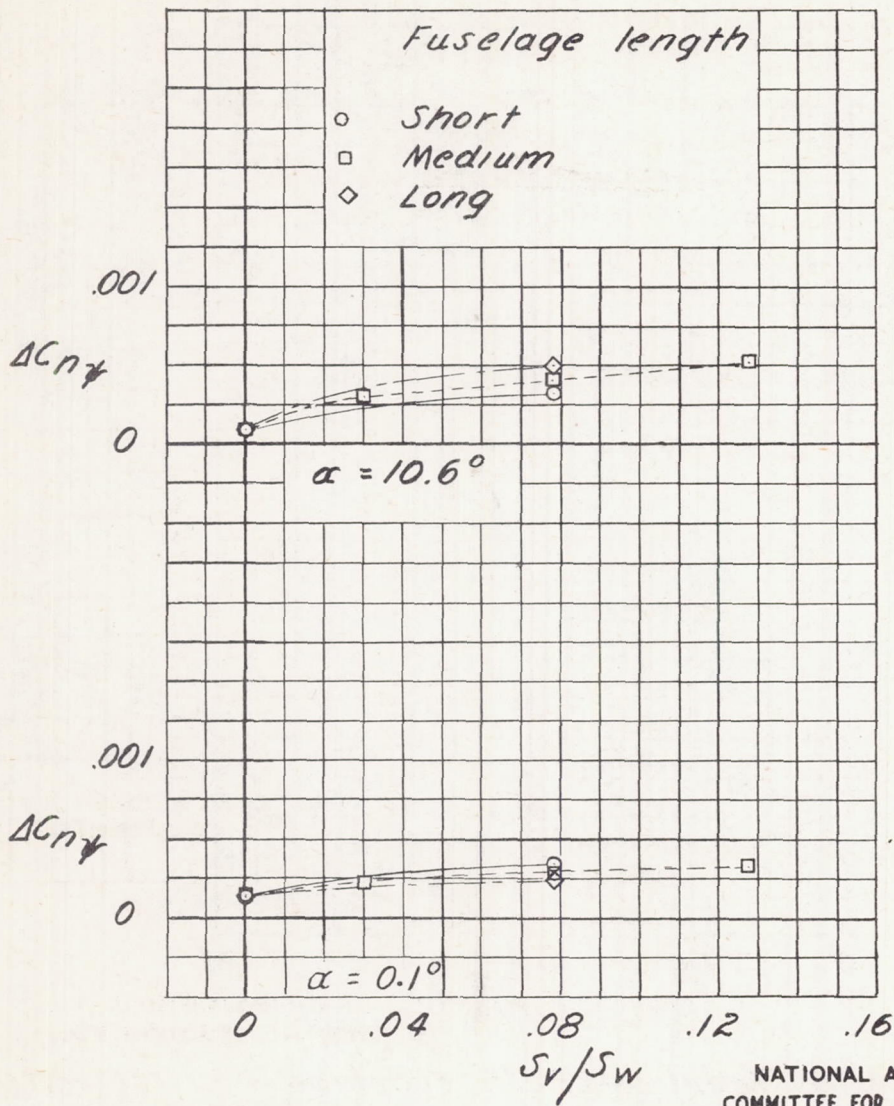


(e) Large box canopy ; short- and long-length fuselage.
 Figure 7. - Concluded.



(a) Medium-length fuselage.

Figure 8 .-Effect of changing vertical-tail area on increment of $C_{n\gamma}$ resulting from addition of canopy to model.



(b) Large box canopy.

Figure 8.- Concluded.

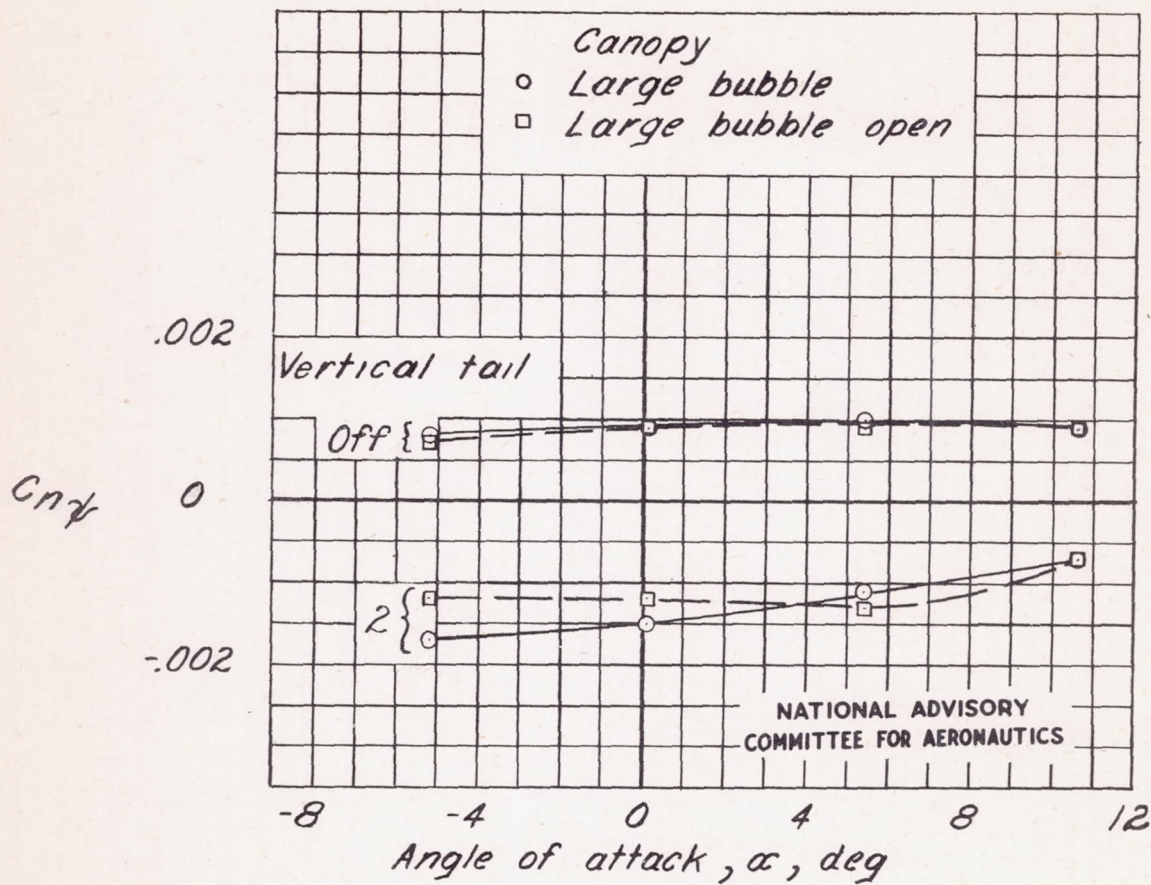


Figure 9.-Effect of opening canopy on variation of lateral-stability derivative $C_{n\gamma}$ with angle of attack. Medium-length fuselage.

